CANADIAN JOURNAL OF RESEARCH

VOLUME 27 MAY, 1949 NUMBER 3

— SECTION A —

PHYSICAL SCIENCES

Contents

Page

The Resonance Method of Measuring the Ratio of the Specific Heats of a Gas, C_p/C_v. Part V. Section A: An Improved Apparatus for Measuring the Ratio of the Specific Heats of a Gas. Section B: The use of Electronic counter Circuits to Measure Low Frequencies and a Variable Low Frequency Oscillator—*L. Katz, S. B. Woods, and W. F. Leverton* 27

The Resonance Method of Measuring the Ratio of the Specific Heats of a Gas, C_p/C_v. Part VI. Carbon Dioxide, Nitrous Oxide, and Methane—*L. Katz, W. F. Leverton, and S. B. Woods* 39

A Recording Meter for Auroral Radiations—*W. D. Penn and B. W. Currie* - - - - - - - - - - - - - 45

Determination of the Elements of Meteor Paths from Radar Observations—*D. W. R. McKinley and Peter M. Millman* - 53

NATIONAL RESEARCH COUNCIL
OTTAWA, CANADA

CANADIAN JOURNAL OF RESEARCH

The *Canadian Journal of Research* is issued in six sections, as follows:

A. Physical Sciences	D. Zoological Sciences
B. Chemical Sciences	E. Medical Sciences
C. Botanical Sciences	F. Technology

For the present, Sections A, C, D, and E are to be issued six times annually, and Sections B and F, twelve times annually, each under separate cover. with separate pagination.

The *Canadian Journal of Research* is published by the National Research Council of Canada under authority of the Chairman of the Committee of the Privy Council on Scientific and Industrial Research. The *Canadian Journal of Research* is edited by a joint Editorial Board consisting of members of the National Research Council of Canada, the Royal Society of Canada, and the Chemical Institute of Canada.

Sections B and F of the *Canadian Journal of Research* have been chosen by the Chemical Institute of Canada as its medium of publication for scientific papers.

EDITORIAL BOARD

Representing
NATIONAL RESEARCH COUNCIL

DR. G. H. HENDERSON, (*Chairman*), Professor of Mathematical Physics, Dalhousie University, Halifax.

DR. A. R. GORDON, Head, Department of Chemistry, University of Toronto, Toronto.

DR. ROBERT NEWTON, President, University of Alberta, Edmonton, Alta.

DR. C. H. BEST, The Banting and Best Department of Medical Research, University of Toronto, Toronto.

Representing
ROYAL SOCIETY OF CANADA

DR. A. NORMAN SHAW, Chairman, Department of Physics, McGill University, Montreal. — Section III

DR. J. W. T. SPINKS, Department of Chemistry, University of Saskatchewan Saskatoon. — Section III

DR. H. S. JACKSON, Head, Department of Botany, University of Toronto, Toronto. — Section V

DR. E. HORNE CRAIGIE, Department of Zoology, University of Toronto, Toronto. — Section V

Ex officio

DR. LÉO MARION, Editor-in-Chief, Division of Chemistry, National Research Laboratories, Ottawa.

DR. H. H. SAUNDERSON, Director, Division of Information Services, National Research Council, Ottawa.

Representing
THE CHEMICAL INSTITUTE OF CANADA

DR. H. G. THODE, Department of Chemistry, McMaster University, Hamilton.

EDITORIAL COMMITTEE

Editor-in-Chief, DR. LÉO MARION
Editor, Section A, DR. A. NORMAN SHAW
Editor, Section B, DR. J. W. T. SPINKS, DR. H. G. THODE
Editor, Section C, DR. H. S. JACKSON
Editor, Section D, DR. E. HORNE CRAIGIE
Editor, Section E, DR. J. B. COLLIP
Editor, Section F, DR. J. A. ANDERSON, DR. A. NORMAN SHAW, DR. H. G. THODE

Manuscripts should be addressed:

Editor-in-Chief,
Canadian Journal of Research,
National Research Council, Ottawa, Canada.

Canadian Journal of Research

Issued by THE NATIONAL RESEARCH COUNCIL OF CANADA

VOL. 27, SEC. A. MAY, 1949 NUMBER

THE RESONANCE METHOD OF MEASURING THE RATIO OF THE SPECIFIC HEATS OF A GAS, C_p/C_v [1]

PART V

SECTION A: AN IMPROVED APPARATUS FOR MEASURING THE RATIO OF THE SPECIFIC HEATS OF A GAS

SECTION B: THE USE OF ELECTRONIC COUNTER CIRCUITS TO MEASURE LOW FREQUENCIES AND A VARIABLE LOW FREQUENCY OSCILLATOR

BY L. KATZ, S. B. WOODS, AND W. F. LEVERTON

Abstract

This paper describes an improved apparatus for the determination of $\gamma = C_p/C_v$, the ratio of the specific heat at constant pressure to the specific heat at constant volume for a gas. With this apparatus, γ is determined by the resonance method of Clark and Katz. The new apparatus is constructed of stainless steel and is designed to withstand pressures up to 100 atm. This new apparatus is more compact and can be used with corrosive gases. Provision is made for the control and accurate measurement of the temperature of the enclosed gas over a wide range of temperatures. An electronic counter which will measure time intervals, in units of 10 μsec., from 100 μsec. to several seconds in length is described in Section B. An unknown frequency may be determined by measuring the time interval in which a preselected number of cycles occurs. The accuracy is such that frequencies may be measured to within approximately 1 part in 10^5. The circuit for a variable frequency transitron oscillator with an output of 30 w. in a range of 15 to 250 c.p.s. is shown. The stability of the oscillator is such that the frequency may easily be maintained within 1 part in 10,000 for long periods, and with care in temperature control and choice of electrode voltages much greater stabilities may be obtained.

Introduction

This paper describes an improved apparatus for the determination of $\gamma = C_p/C_v$, the ratio of the specific heat at constant pressure to the specific heat at constant volume of gases. With this apparatus γ is determined by the resonance method (5, 6, 7). This consists essentially of a determination of the resonant frequency of a piston separating equal volumes of the gas at the desired pressure and temperature.

The new apparatus is designed to operate at pressures up to 100 atm. The temperature can be determined accurately and controlled over a range from -40 to $+100°$ C. This is in strong contrast to the old apparatus, which operated only at temperatures in the immediate neighborhood of room temperature (5).

[1] *Manuscript received in original form September 14, 1948, and, as revised, January 20, 1949. Contribution from the Department of Physics, University of Saskatchewan, Saskatoon, Sask.*

The ratios of specific heats at zero pressure have been determined from spectroscopic data for many monatomic and diatomic gases, and more recently, for triatomic and a few more complicated gases. The latter calculations are extremely involved and depend upon the proper assignment of fundamental frequencies to the molecule. Our results upon extrapolation to zero pressure should serve as a check on the spectroscopic work, especially in the case of triatomic and higher order molecules. Such a check is desirable because spectroscopists use these same fundamental frequencies to calculate moments of inertia and internuclear distances of the various molecules.

Clark and Katz (4) have described an accurate method of measuring low frequencies which requires a darkroom and necessitates the development of photographs before the frequency is known. While engaged in wartime research, the senior author of the present paper employed several electronic counter circuits and recognized their application to frequency measurement. With such a counter the frequency is obtained immediately by means of one simple arithmetical operation.

The dynatron oscillator described by Clark and Katz (4) for the production of low frequency currents has been replaced by a transitron oscillator. The latter type of oscillator is not critical to electrode voltages nor to individual tube characteristics. It will operate over an extended range of frequencies with good stability and provide an excellent laboratory oscillator where elaborate circuits are not desirable.

Simple and accurate methods of calibrating the frequency meter and testing the operation of the meter and oscillator, using the standard signals broadcast by WWV, the Washington Bureau of Standards transmitter, have been employed.

Section A

Mechanical Design of the New Apparatus

Theoretical considerations on which the design of a sharply resonant system is based were outlined in a previous paper (5). The present apparatus was constructed with these limitations in mind. The values of the pertinent design factors are, approximately:

Gas volume	34 cm.^{3}
Piston mass	95 gm.
Piston area	7.9 cm.^{2}
Range of resonant frequency	
at 1 atm.	45 c.p.s.
at 20 atm.	180 c.p.s.

The general outline of the new apparatus is shown in Fig. 1. The piston (P) was made of stainless steel type 410 (S.A.E.). This steel is ferromagnetic. The inner cylinder (C_1) was made of stainless steel type 330, which is non-magnetic. Both types are noncorrosive, thus making it possible to use the

apparatus for the study of gases such as chlorine. These materials have nearly equal coefficients of thermal expansion,

Type	Coefficient of expansion/°C.
410	10.9×10^{-6}
330	11.3

making it possible to use the apparatus over a wide range of temperatures with little change in the clearance between piston and cylinder.

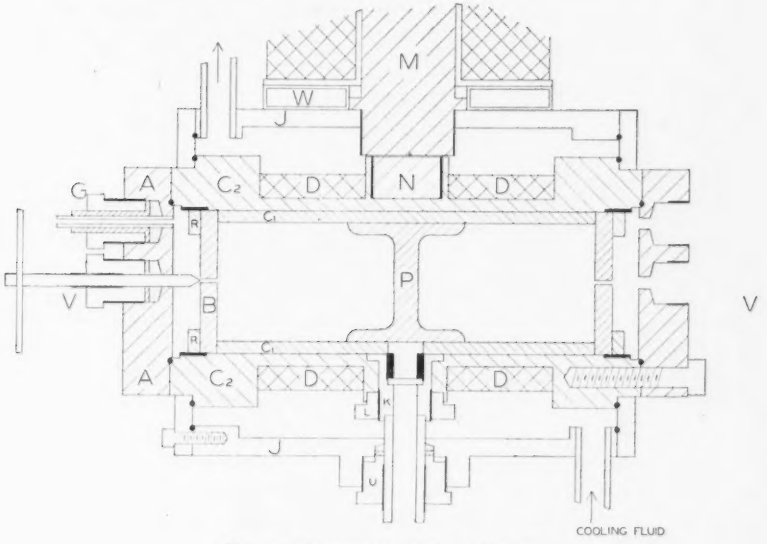

FIG. 1. *Construction of the apparatus*

Piston and cylinder must fit very closely (all around clearance of a few ten-thousandths of an inch) in order that error due to excessive gas leakage past the piston will be avoided. This necessitated that both piston and inner cylinder surface be machined round to a very fine tolerance. Further, friction must be kept to a minimum, thus requiring that these surfaces be very smooth. The piston was lightly plated with chromium to give a good wearing surface and to reduce the possibility of the piston's sticking. The ends of the resonator cylinder must be flat and parallel to ensure that the end plates (B, B) form a good seal and to make possible an accurate determination of the volume of the enclosed gas.

The diameter of the piston and the length of the resonator cylinder were measured by means of a set of gauge blocks accurate to $\pm$ 4 $\times$ 10^{-6} in. and a comparator with smallest divisions equivalent to 50 $\times$ 10^{-6} in. The mean clearance of the piston within the cylinder, and hence the inside diameter of

the cylinder, was determined by measuring the rate of gas leakage past the piston under a known pressure head. The mean all around clearance was found to be 3.3×10^{-4} in.

A fine scratch was machined around the piston midway along its length. Observation of the amplitude of motion of this scratch when the piston is oscillating enables one to determine the resonance frequency.

The outer cylinder (C_2), of noncorrosive, nonmagnetic stainless steel, serves as the high pressure container. It carries the coils (D) through which an alternating current is passed to drive the piston. Each coil consists of 5900 turns of No. 34 enamelled copper wire. (R,R) are rings to hold the end plates of the resonating chamber in place. The outer end plates (A,A) serve to seal off the pressure cylinder. These end plates also carry the gas inlets (G,G) and the inlet valves (V,V).

(J) is a brass cylinder. The annular space between this cylinder and the pressure cylinder is closed off at the ends by brass rings. Oil circulated through this space controls the temperature of the apparatus.

(M) is an electromagnet. The current through the electromagnet coil is adjusted so that the force on the piston due to the magnet is just sufficient to counterbalance the force due to gravity. This causes the piston to "float" in the cylinder and greatly reduces the friction. (N) is a plug of ferromagnetic material tapped into the pressure cylinder wall directly below the core of the lift magnet. Its purpose is to extend the core of the lift magnet nearer to the piston. Water may be circulated through the hollow brass ring (W) to reduce the flow of heat from the lift magnet coil to the apparatus.

Directly opposite the lift magnet, a glass window is sealed into the wall of the pressure cylinder to permit observation of the motion of the piston. The window is sealed into the boss (K) between "silastic" washers. The nut (L) holds K in position. A brass tube and boss (U) provide a clear optical path through the cooling chamber.

Fig. 2 shows the optical system used to view the motion of the piston in the apparatus. A beam of light from a projection lamp is reflected vertically

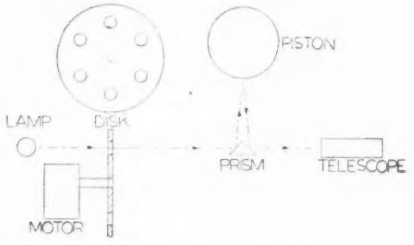

FIG. 2. *Optical system.*

upward by one face of a small 90 degree aluminized glass prism. The light passes through the window, is reflected by the piston surface, and returns

through the window to the prism. Part of the returning beam is reflected out horizontally by the second face of the prism into the telescope.

A wooden disk with six uniformly spaced $\frac{1}{2}$ in. holes near its circumference is placed between the light source and the prism. By adjusting the rate of rotation of the disk, i.e., the number of interruptions of the light beam, to match the frequency of the piston, the apparent motion of the latter can be made as slow as desired stroboscopically and the amplitude of its excursion measured with precision.

Temperature Control

The apparatus is maintained at any desired temperature by circulating oil from a thermostatically controlled tank through the outer jacket. The temperature of the interior of the apparatus is determined as follows. A copper-constantan junction is set in the wall of the pressure cylinder (C_2) and is connected through a sensitive galvanometer to a similar junction which is suspended in the oil tank near the bulb of a thermometer. The thermometer indicates the temperature of the oil in the tank and the galvanometer deflection gives the difference between this and the temperature of the apparatus. We are able to maintain and determine the temperature of the apparatus within 0.05° C.

Determination of γ

In the earlier papers (5, 6, 7) it was shown that:

$$\gamma = \frac{m V_0 \omega_m^2}{2a^2 P_0} \Lambda \chi G \Gamma,$$

where m = mass of piston,

V_0 = volume of gas on either side of piston,

ω_m = frequency at maximum amplitude of piston motion,

a = effective area of end of piston,

P_0 = pressure of gas,

$\Lambda = \frac{m + m_g}{m}$, where m_g is the mass of a volume V_0 of the enclosed gas,

χ = correction for the effect of friction between piston and cylinder,

G = correction for nonideal behavior of the gas,

Γ = correction for nonadiabatic change of the gas.

The pressure is measured by means of a mercury and glass manometer up to 6 atm., and at higher pressures by means of the Amagat gauge used in the earlier work.

The alternating current to drive the piston is supplied by a transitron oscillator of very high stability. The oscillator and the method of measuring its frequency are described in Section B of this paper.

Performance of the New Apparatus

This method is absolute in the sense that it is not necessary to calibrate the apparatus by means of measurements with a gas for which γ is already known. The different correction factors involved are also obtained from the experimental set-up and various quantities which can be calculated. In order to check the functioning of the new apparatus and the values of the constants m, V_0, and a, a series of measurements was made of γ at various pressures from 1 to 5 atm. for argon. A straight line was fitted to the experimental points (γ vs. pressure) by the method of least squares. The mean variation of the experimental points from this straight line was 0.06%. Extrapolation yielded $\gamma = 1.6662$ at zero pressure. This differs by 0.03% from $\gamma = 1.667$ obtained previously by this method and also by the spectroscopic method.

Section B

The Electronic Frequency Meter and Interval Timer

Electronic counter circuits and associated equipment for their use in many applications have been described in the literature recently. The complete circuits for an instrument suitable to use as a frequency meter have not yet appeared.

The block diagram of Fig. 3 shows the sequence of operation of the circuits in the meter. The signal of unknown frequency is connected to a pulse

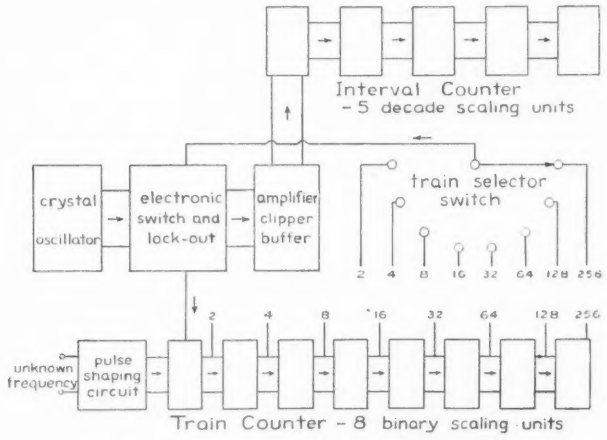

FIG. 3. *Block diagram of the frequency meter.*

forming circuit, the output of which has the same wave form irrespective of the input wave form. The output is then applied to the train counter, which consists of eight scale-of-two frequency dividing circuits. The output of

any one of these scaling circuits may be chosen, by means of the train selector switch, to operate the electronic switch. When the first pulse is received by the electronic switch, a gate circuit opens, allowing the pulses from the 100 kc. crystal oscillator to be counted and recorded by the interval counter. The next pulse closes the gate so that the 100 kc. pulses are no longer counted. The lockout circuit operates at the same time and prevents further operation of the meter until it is manually reset. The number of cycles of the 100 kc. oscillator that occurred in the time interval between the pulses which operated the electronic switch is recorded by means of neon lights on the interval timer. This corresponds to a train of 2, 4, 8, 16, 32, 64, 128, or 256 cycles of the unknown frequency, depending on the position of the train selector switch. Dividing the number of cycles in the train by the time interval during which they occurred, as indicated by the neon lights of the interval counter, gives immediately the frequency of the source.

Figs. 4, 5, 6, and 7 are the diagrams of the circuits used in the counter. V. H. Regener (12) discusses thoroughly the choice of design parameters for the pulse forming circuit used here. The frequency scaling stages of the train counter use the circuit originally developed by Eccles and Jordan (8) and modified by Potter (10, 11). The action of dual triode trigger pairs such as this circuit employs is described by B. E. Phelps (9). The electronic switch employs a similar circuit. The potentials shown in Fig. 6 are those obtained with the gate circuit in the closed condition. The decade frequency scaling circuits used in the interval counter were developed by Potter (10, 11) and are described by him together with the method of reading the neon lights. G. T. Baker (1) discusses a method of design procedure for this circuit. The method used by Regener (12) may also be adapted for use with triode trigger circuits such as employed in the interval and train counters.

A Bliley Type FM6-S 100 kc. standard frequency crystal, with the oscillator circuit suggested by the manufacturers is used as the standard source. This oscillator maintains a frequency stability of $\pm$ 0.005% over a temperature range of 0 to 50° C.

The oscillator was calibrated by beating the fiftieth harmonic of its output against the 5 megacycle carrier broadcast from WWV. A wire carried from the output of the 6AG7 clipper amplifier alongside the antenna of a receiver tuned to WWV radiated enough energy to produce the beat note. In this manner, the oscillator could be adjusted to within one part in five million of the WWV signal. Subsequent checks over a period of a year showed it always to be within one part in one million of this frequency.

Since the gate circuit may open part way through a cycle of the standard oscillator which will not be counted or close part way through a cycle which is already counted there may be an error of $\pm$ 1 count in the reading of the interval counter. This represents an error of $\pm$ 10 μsec. in the measurement of the time interval, which should normally be the largest error.

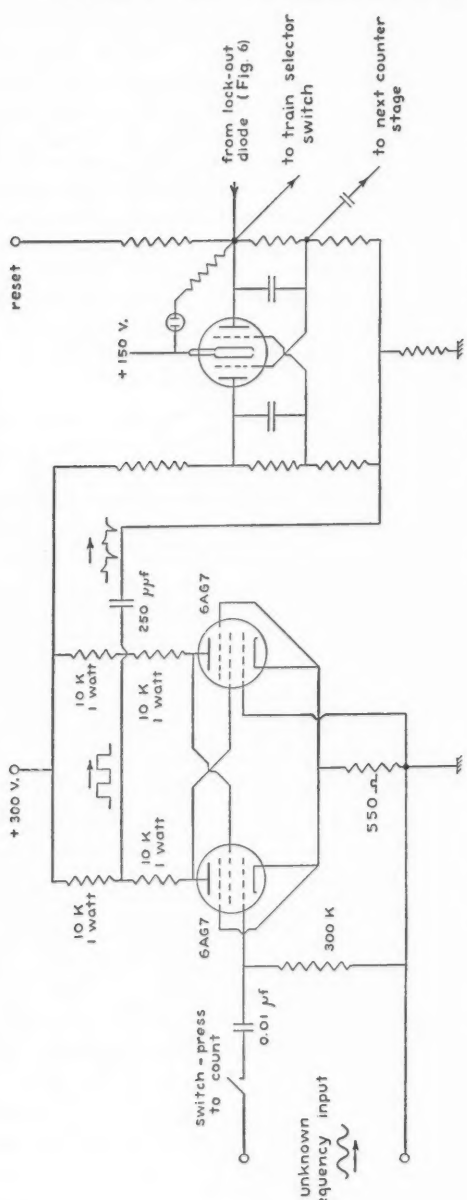

FIG. 4. *Pulse forming circuit and the first stage of the train counter. All resistors are ½ w. unless otherwise specified.*

If a well filtered power supply is employed, dependable operation is obtained with voltage variations of ± 10% without special regulation equipment. The total power consumption is less than 150 w.

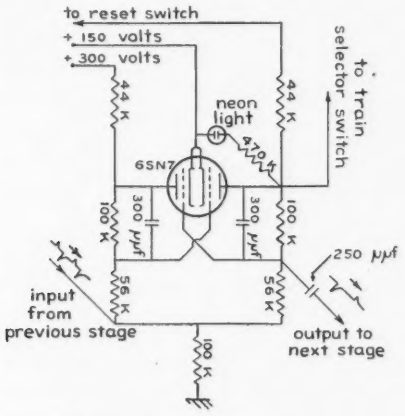

FIG. 5. *Binary frequency scaling unit. All resistors are ½ w.*

TRANSITRON OSCILLATOR

The oscillator with a three stage amplifier is shown in Fig. 8. For stability the oscillator is powered entirely by batteries and very lightly coupled to the amplifier. The correct voltages were located experimentally and are not critical. The tuned circuit consists of the inductance and condensers used by Clark and Katz (4). At low frequencies a resistance in series with the tuned circuit is necessary to satisfy the conditions for oscillation given by Brunetti (2, 3). The amplifier has been changed only slightly from that shown by Clark and Katz, in order to obtain greater power output.

MEASUREMENTS AND RESULTS

The consistency of the results obtained when measuring the frequency of the transitron oscillator with the meter was used as a test of their combined performance. Both the oscillator and counter were allowed a one hour warm-up period before the readings were taken. Ten measurements were made at each of 22 different frequencies between 25 and 250 c.p.s. The maximum departure of any reading from the mean value for the 10 trials was always less than 0.01% and, for several frequencies, corresponded to an error of 10 μsec. in the measurement of the time interval.

To ensure that there was no systematic error in the determinations, a known frequency was obtained and measured. A receiver was tuned to WWV on 5 megacycles and the output of the audio amplifier, which contained the standard frequency of 440 c.p.s., was connected to the vertical plates of an

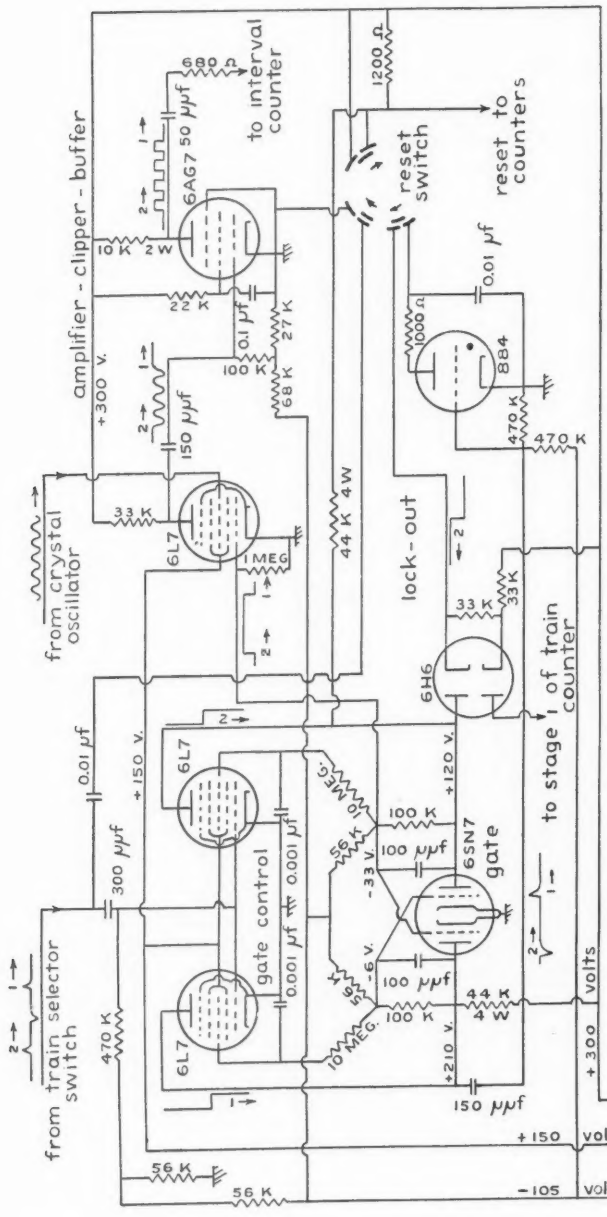

FIG. 6. *Electronic switch, lockout and amplifier-clipper-buffer circuits. All resistors are ½ w. unless otherwise specified.*

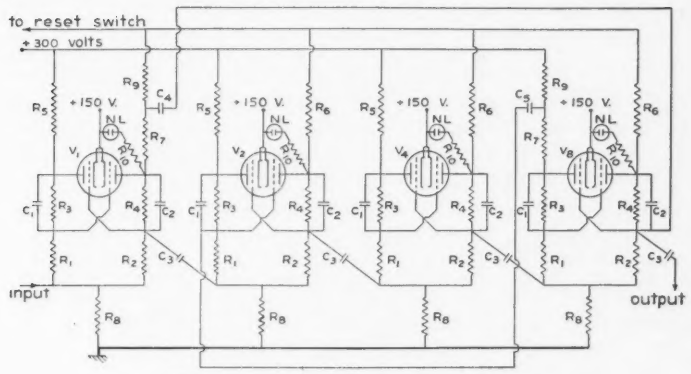

FIG. 7. *Decade frequency scaling unit.*

R_1, R_2	56,000 ohms
R_3, R_4, R_8	100,000 ohms
R_5, R_6	44,000 ohms
R_7, R_9	22,000 ohms
R_{10}	470,000 ohms

All resistors are $\frac{1}{2}$ *w.*

C_1, C_2	300 μμf.
C_3	500 μμf.
C_4	50 μμf.
C_5	100 μμf.

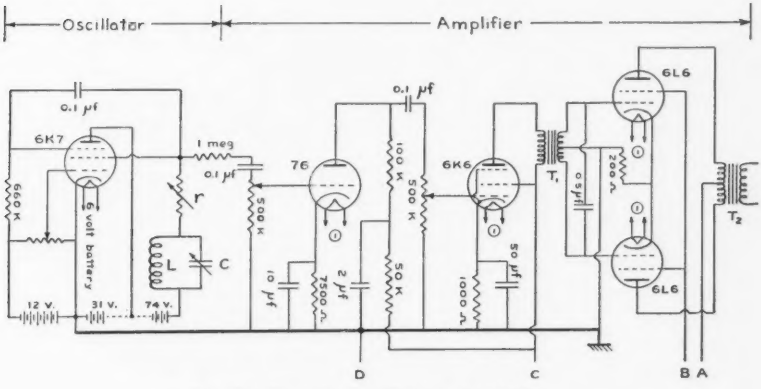

FIG. 8. *Transitron oscillator and amplifier*

L	10 h., 130 ohm, air core.
C	0 to 10 μf. variable condenser.
r	0 to 3000 ohms.
T_1 P	11,000 ohms
T_1 $S/2$	690 ohms
T_2 P	5000 ohms
T_2 S	5000 ohms
A 420 v., B 360 v., C 280 v., D 0 v.	to power supply.

oscilloscope. The output of the transitron oscillator was connected to the horizontal plates of the oscilloscope and a static Lissajous figure was obtained by adjusting the frequency of the transitron to 220 c.p.s. This adjustment was repeated several times, and each time the frequency was measured, using a number of different train lengths. The maximum departure of any of these readings from 220.000 cycles per second was 0.009%, which is within the accuracy with which the Lissajous pattern could be set.

References

1. BAKER, G. T. J. Sci. Instruments, 25 : 194. June, 1948.
2. BRUNETTI, C. Proc. Inst. Radio Engrs. 25 : 1595. 1937.
3. BRUNETTI, C. Proc. Inst. Radio Engrs. 27 : 88. 1939.
4. CLARK, A. L. and KATZ, L. Can. J. Research, A, 16 : 183. 1938.
5. CLARK, A. L. and KATZ, L. Can. J. Research, A, 18 : 22. 1940.
6. CLARK, A. L. and KATZ, L. Can. J. Research, A, 19 : 111. 1941.
7. CLARK, A. L. and KATZ, L. Can. J. Research, A, 21 : 1. 1943.
8. ECCLES, W. H. and JORDAN, F. W. Radio Rev. 1 : 143. 1919.
9. PHELPS, B. E. Electronics, 18 : 110. July, 1945.
10. POTTER, J. T. Electronics, 17 : 110. June, 1944.
11. POTTER, J. T. Electronics, 17 : 358. June, 1944.
12. REGENER, V. H. Rev. Sci. Instruments, 17 : 180. 1946.

THE RESONANCE METHOD OF MEASURING THE RATIO OF THE SPECIFIC HEATS OF A GAS, C_p/C_v

VI. CARBON DIOXIDE, NITROUS OXIDE, AND METHANE

By L. Katz, W. F. Leverton, and S. B. Woods

Abstract

Carbon dioxide, nitrous oxide, and methane have been carefully purified and the variation of γ with pressure measured. The results when extrapolated to zero pressure give values of γ_0 which are in agreement with those obtained by spectroscopic methods. Agreement in each case is better than 0.10%.

Carbon Dioxide

The variation of γ, the ratio of the specific heats, with pressure was measured previously for carbon dioxide by this method (1). Upon extrapolation of the results to zero pressure it was found that the value of γ_0 was higher than that obtained by the spectroscopic method by 0.49% (3).

Since the probable error in the zero pressure value of γ by this method is less than 0.10%, it was felt that the large difference might have been due to the presence of impurities in the carbon dioxide.

For the present experiment carbon dioxide 99.5% pure was obtained from a commercial source and a careful purification undertaken. The impurities were air and water vapor. The gas was purified by a fractional distillation over liquid air, the first and last tenth being discarded at each stage. γ was measured for a sample which had been put through a three stage distillation. The zero pressure value was found to be 0.10% higher than the spectroscopic value. The results given in Table I were obtained using a sample of carbon dioxide which had been given a five stage distillation.

The $Pv-P$ data of Michels (7) used previously (1) was employed in calculating Λ and G. The constants of the apparatus were as follows.

Mass of piston = 95.448 gm.
Volume of enclosed gas = 34.053 cm.^{3}
Effective area of end of piston = 7.9169 cm.^{2}

Substitution of these in the equation for γ developed previously (5) yields

$$\gamma = 1.0102 \times 10^{-3} \frac{f_m^2}{P_0} \Lambda \chi G \Gamma$$

where f_m is in cycles per second and P_0 is in standard atmospheres.

[1] *Manuscript received in original form September 14, 1948, and, as revised, January 26, 1949.*

Contribution from the Department of Physics, University of Saskatchewan, Saskatoon, Sask.

TABLE I

CARBON DIOXIDE (29.9° C.)

Pressure, atm.	Resonance frequency, c.p.s.	Λ	G	χ	Γ	γ	$\gamma_{equa.}$	$\gamma - \gamma_{equa.} \times 10^4$
1.2283	39.416	1.0008	1.0060	1.0004	1.0061	1.2948	1.2934	+14
1.7514	47.027	1.0011	1.0086	1.0001	1.0047	1.2942	1.2967	−25
2.1315	51.953	1.0014	1.0105	1.0001	1.0040	1.2998	1.2991	+ 7
3.6082	67.578	1.0023	1.0181	1.0001	1.0027	1.3084	1.3084	0
4.3076	73.849	1.0028	1.0219	1.0001	1.0024	1.3140	1.3128	+12
5.1330	80.537	1.0033	1.0260	1.0001	1.0021	1.3170	1.3180	−10
6.2058	88.513	1.0041	1.0320	1.0001	1.0019	1.3242	1.3247	− 5
7.2744	95.852	1.0048	1.0381	1.0001	1.0017	1.3333	1.3315	+18
8.2250	101.766	1.0054	1.0434	1.0001	1.0015	1.3365	1.3374	− 9

The results were fitted by the method of least squares, giving the equation

$$\gamma_{equa.} = 1.2857 + 6.29 \times 10^{-3}P \ . \qquad (1)$$

The last column of Table I shows the differences between experimental values of γ and those calculated using Equation (1). The mean difference is 0.0011 or approximately 0.08%. Extrapolation of Equation (1) to zero pressure yields $\gamma_0 = 1.285_7$. The spectroscopic method (4) yields $\gamma_0 = 1.2857$ at zero pressure and the same temperature, 29.9° C. The difference is 0.00%. The experimental results and the least squares equation are plotted in Fig. 1.

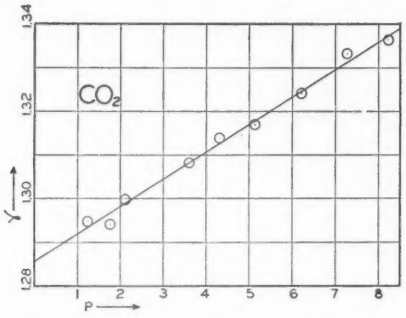

FIG. 1. *Ratio of specific heats for carbon dioxide as a function of pressure, at 29.9° C.*

Nitrous Oxide

Gamma has been determined previously for nitrous oxide (2) but at zero pressure the resulting value was 0.38% higher than that obtained by the spectroscopic method (3). A supply of nitrous oxide of 98 to 99% purity was obtained, the impurity being nitrogen. The gas was put through a five stage distillation similar to that employed with carbon dioxide. Table II shows the results obtained.

TABLE II

NITROUS OXIDE (25.3° C.)

Pressure, atm.	Resonance frequency, c.p.s.	Λ	G	χ	Γ	γ	$\gamma_{equa.}$	$\gamma-\gamma_{equa.}\times 10^4$
1.4017	38.943	1.0007	1.0081	1.0002	1.0049	1.2795	1.2794	+ 1
1.6944	42.816	1.0009	1.0098	1.0002	1.0043	1.2811	1.2810	+ 1
1.8877	45.177	1.0010	1.0109	1.0002	1.0040	1.2813	1.2821	− 8
2.3101	49.986	1.0013	1.0134	1.0003	1.0033	1.2845	1.2848	− 3
2.6944	54.005	1.0015	1.0158	1.0002	1.0031	1.2884	1.2876	+ 8
2.9757	56.755	1.0016	1.0175	1.0002	1.0029	1.2906	1.2897	+ 9
3.6897	63.165	1.0025	1.0219	1.0001	1.0026	1.2954	1.2959	− 5
4.8102	72.156	1.0033	1.0290	1.0001	1.0022	1.3061	1.3077	−16
5.3356	76.118	1.0037	1.0325	1.0001	1.0020	1.3152	1.3141	+11

The constants of the apparatus were as follows:

Mass of piston = 114.361 gm.

Volume of enclosed gas = 32.808 cm.^{3}

Effective area of end of piston = 7.9165 cm.^{2},

whence $\gamma = 1.1663 \times 10^{-3} \frac{f_m^2}{P_0} \Lambda\chi G\Gamma$.

We used the same $Pv-P$ data as used previously (2). The results were fitted by the method of least squares to the following second order equation

$$\gamma_{equa.} = 1.2744 + 2.25 \times 10^{-3}P + 9.73 \times 10^{-4}P^2 . \qquad (2)$$

The last column of the table shows the differences between experimental values of γ and those calculated using Equation (2). The mean difference is 0.0007 or 0.05%. Equation (2) yields a zero pressure value $\gamma_0 = 1.274_4$. The spectroscopic method (4) yields $\gamma_0 = 1.2733$ at the same temperature, 25.3° C. Our value differs from the spectroscopic value by 0.0011 or 0.09%. The experimental results and the least squares equation are plotted in Fig. 2.

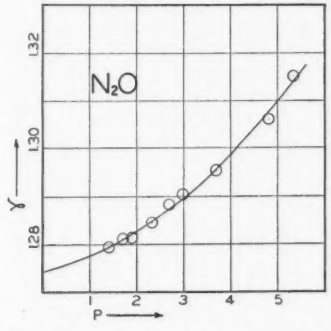

FIG. 2. *Ratio of specific heats for nitrous oxide as a function of pressure, at 25.3° C.*

Methane

Methane of 99% purity was obtained and was purified by the previously described five stage distillation over liquid air. The $Pv-P$ data of Keyes and Burks (6) was used in calculating Λ and G. The apparatus constants were the same as for nitrous oxide. The results for methane are shown in Table III.

TABLE III

METHANE (25.1° C.)

Pressure, atm.	Resonance frequency, c.p.s.	Λ	G	χ	Γ	γ	$\gamma_{equa.}$	$\gamma-\gamma_{equa.}\times 10^4$
1.5471	41.319	1.0003	1.0027	1.0003	1.0086	1.3023	1.3025	− 2
2.0435	47.517	1.0004	1.0036	1.0002	1.0070	1.3031	1.3028	+ 3
2.5402	52.973	1.0005	1.0045	1.0002	1.0059	1.3026	1.3033	− 7
3.2130	59.633	1.0006	1.0057	1.0002	1.0050	1.3056	1.3045	+11
3.6238	63.317	1.0007	1.0064	1.0002	1.0046	1.3056	1.3055	+ 1
3.9704	66.295	1.0008	1.0070	1.0001	1.0043	1.3068	1.3063	+ 5
4.4032	69.788	1.0008	1.0078	1.0002	1.0040	1.3066	1.3077	−11
4.8240	73.086	1.0009	1.0086	1.0001	1.0037	1.3086	1.3091	− 5
5.2965	76.646	1.0010	1.0094	1.0001	1.0034	1.3117	1.3109	+ 8

The experimental values of γ, at 25.1° C., were fitted by the method of least squares by the following equation:

$$\gamma_{equa.} = 1.3029 - 1.05 \times 10^{-3}P + 4.84 \times 10^{-4}P^2 . \qquad (3)$$

Table III also shows the differences between experimental values of γ and those calculated using Equation (3). The mean difference is 0.0006 or 0.05%. Equation (3) yields a zero pressure value $\gamma_0 = 1.302_9$.

Using the value of C_{p_0} obtained by Vold (8) by the spectroscopic method, the zero pressure value of γ at the same temperature (25.1° C.) is 1.303_0. These values differ by 0.0001 or 0.01%. The experimental results and the least squares equation are plotted in Fig. 3.

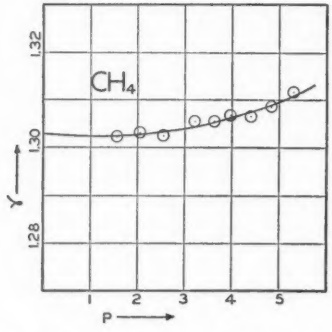

FIG. 3. *Ratio of specific heats for methane as a function of pressure, at 25.1° C.*

It is of interest to note that Vold sets an upper limit of 3% on the error in his value of C_{p_0}. An error of 3% in C_{p_0} introduces an error of 0.9% in γ_0. The excellent agreement of our zero pressure value with that using Vold's results indicates that his values of C_{p_0} for methane are probably accurate to within a few tenths of one per cent.

Summary

Table IV gives a summary of results by the resonance method, together with results obtained by spectroscopic methods by various observers.

TABLE IV

SUMMARY OF RESULTS

Gas	Temp., ° C.	γ, Present work		γ_0, Spectroscopic methods, 0 atm.	Diff. %
		1 atm.	0 atm.		
CO_2	29.9	1.292_0	1.285_7	1.2857 (4)	0.00
N_2O	25.3	1.277_6	1.274_4	1.2733 (4)	+0.09
CH_4	25.1	1.302_3	1.302_9	1.303_0 (8)	−0.01

References

1. CLARK, A. L. and KATZ, L. Can. J. Research, A, 18 : 22. 1940.
2. CLARK, A. L. and KATZ, L. Can. J. Research, A, 19 : 111. 1941.
3. CLARK, A. L. and KATZ, L. Can. J. Research, A, 21 : 1. 1943.
4. KASSEL, L. S. J. Am. Chem. Soc. 56 : 1838. 1934.
5. KATZ, L., WOODS, S. B., and LEVERTON, W. F. Can. J. Research, A, 27 : 27. 1949.
6. KEYES, F. G. and BURKS, H. G. J. Am. Chem. Soc. 49 : 1403. 1927.
7. MICHELS, A. and MICHELS, C. Proc. Roy. Soc. (London), A, 153 : 201. 1935.
8. VOLD, R. D. J. Am. Chem. Soc. 57 : 1192. 1935.

APPENDIX

Effect of Impurities

For a mixture of n gases, containing $m_1, m_2 \ldots\ldots m_n$ moles of the different gases, the ratio of specific heats may be calculated as follows:

The heat absorbed by the mixture per degree centigrade rise in temperature at constant volume is given by

$$(DQ)_v = mC_{v\,mix} = \sum_1^n m_j C_{v\,j}\ , \qquad (1)$$

where $m = \sum_1^n m_j$. This equation assumes that there is no interaction between the molecules of the different gases.

Now, from thermodynamics,

$$C_{pj} - C_{vj} = T\left(\frac{\partial P}{\partial T}\right)_v \left(\frac{\partial V}{\partial T}\right)_P = R_j \,, \tag{2}$$

where R_j depends on the gas, temperature, and pressure, but is equal to the gas constant, R, at zero pressure.

Dividing each side by C_{vj}

$$\frac{C_{pj} - C_{vj}}{C_{vj}} = \gamma_j - 1 = \frac{R_j}{C_{vj}} \,, \tag{3}$$

or

$$C_{vj} = \frac{R_j}{\gamma_j - 1} \,.$$

Introducing this into Equation (1) we have

$$\frac{R_{mix}}{\gamma_{mix} - 1} = \sum_1^n \frac{r_j R_j}{\gamma_j - 1} \,, \tag{4}$$

where

$$r_j = \frac{m_j}{m} \,.$$

At zero pressure, $R_j = R_{mix} = R$

and

$$\gamma_{mix.,\,0} = 1 + \frac{1}{\sum_1^n \frac{r_j}{\gamma_j - 1}} \tag{5}$$

For a mixture of two components, where $r_1 \gg r_2$

$$\gamma_{mix.,\,0} = \gamma_1 + r_2 (\gamma_2 - \gamma_1)\left(\frac{\gamma_1 - 1}{\gamma_2 - 1}\right) \,.$$

Change in γ of carbon dioxide caused by 1% by weight of various impurities:

Impurity	% change in γ
H_2	+ 1.2
He	+ 1.3
A	+ 0.14
N_2	+ 0.10
O_2	+ 0.09
Air	+ 0.10

A RECORDING METER FOR AURORAL RADIATIONS[1]

By W. D. Penn and B. W. Currie

Abstract

This paper describes a device that was developed to give a continuous record of the intensity of auroral radiations from the zenithal sky. Detection is by means of the multiplier phototube, R C A type 1P21. A null method of recording is used, the light flux reaching the phototube being kept to a constant value by moving a neutral, wedge filter in front of the phototube. A simple servomechanism is used for this purpose. A pen attached to the filter traces a record of the changes of auroral intensity on a clock-driven chart.

Introduction

The development of a convenient, mechanical device for recording the occurrence and intensity of auroras is a necessity, if progress is to be made in deducing reliable diurnal and annual variations of auroras and in detecting significant relations between auroral variations and magnetic, earth-current, and ionospheric disturbances. The visual observations, presently available, suffer from at least three faults that are inherent in using human instead of mechanical detectors and recorders. The first is a lack of continuity, since most observatories never have sufficient staff to keep a continuous watch on the night sky; the second arises from the inability of an observer to record more than a small fraction of the apparent auroral changes during active displays; and the third results from the lack of comparative standards of brightness and intensity, an observer having to depend on his previous experiences and his judgment in making estimates of these quantities.

Objective methods of recording auroral occurrence and intensity require the use of either photographic or photoelectric detectors. With photographic detectors the exposure times must be sufficiently long to make possible reliable measurements of the blackening of the emulsion. For the majority of displays, this condition requires exposures over periods that are long in comparison with the times for the more rapid changes in geomagnetic disturbance. However, the photographic method has been, and is, used to a limited extent (2, 3, 4), either the plate on a spectrograph being moved slowly parallel to the slit or a film being moved slowly past a narrow slit through which can pass the auroral radiations from a particular region of the sky. While photoelectric detectors respond almost instantaneously to changes of flux, the currents induced by the auroral radiations are so small that they require considerable amplification to operate a recorder. Until the development of multiplier phototubes, this meant the use of fairly involved electronic circuits that evidently could not be operated satisfactorily under the conditions usually

[1] *Manuscript received November 8, 1948.*

Contribution from the Physics Department, University of Saskatchewan, Saskatoon, Sask. This paper was presented at the General Assembly of the International Union of Geodesy and Geophysics at Oslo, Norway, August 19-28, 1948.

prevailing at high-latitude observatories. In any case, no systematic study of the records from such a device has appeared in auroral literature, although the use of the records has been mentioned (6).

Gartlein (1) has operated a photoelectric recorder, using a multiplier phototube, at Ithaca, New York State, for several years. This recorder apparently uses a rotating sectored disk to pulse the radiations incident on the phototube, an alternating current amplifier, a rectifier, and a recorder. The writers have operated a photoelectric recorder, also using a multiplier phototube, at Saskatoon, Saskatchewan (52° 6′ N., 100° 36′ W.). It makes use of a null method of recording, the flux on the phototube being kept substantially constant by using a servo-mechanism to move a neutral wedge filter backward and forward in front of the phototube. The results to date indicate that a great deal of useful information concerning auroral intensities (the integrated effect of brightness over a particular region of the sky), can be secured by this device, or by modification of it, for correlation with various types of geomagnetic disturbance.

Details of the Recorder

One of the most sensitive photoelectric detectors of low light fluxes available is the tube referred to as R C A Type 1P21. It has an average current amplification factor of 1.2×10^6 for a power supply of 100 v. per dynode stage. This large amplification makes it particularly suitable for detecting the smallest auroral fluxes, since with it there is a minimum need for external amplifying units that not only add to the bulk of the recorder but increase the possibility of an unfavorable signal-to-noise ratio. However, it is subject to a fatigue in the later and higher-current stages that increases rapidly for increasing output currents above 10 μa. This is a matter of some concern in using this type of phototube in an auroral recorder, since the recorder should yield reliable values of light fluxes ranging from those of the twilight sky to those of the normal night-sky when covered with cloud. Assuming a brightness of 10^{-8} candles per cm.^{2} for the night-sky, an effective reduction of this quantity by a factor of 10^{-2} by cloud, and a brightness of 10^{-5} candles per cm.^{2} for the zenithal sky when the sun is 8° below the horizon, the maximum flux on the phototube amounts to 10^5 times the minimum flux.

Two methods may be used to control the output current at times of high light flux. One is to reduce the dynode voltage by the plate-cathode current of a control tube, the grid voltage of which is dependent on the current from the phototube (5), and the other is to reduce the light flux incident on the phototube by moving a wedge filter between the phototube and the sky. The latter method was adopted, since the changes of light flux could be conveniently recorded by attaching a pen to the filter and having it leave a trace on a clock-driven chart.

A simple servo-mechanism is used to move the filter. The circuit diagram for the recorder (including the servo-mechanism), is shown in Fig. 1. The voltage drop across a 1-megohm resistor (R_{13}) in the anode circuit of the

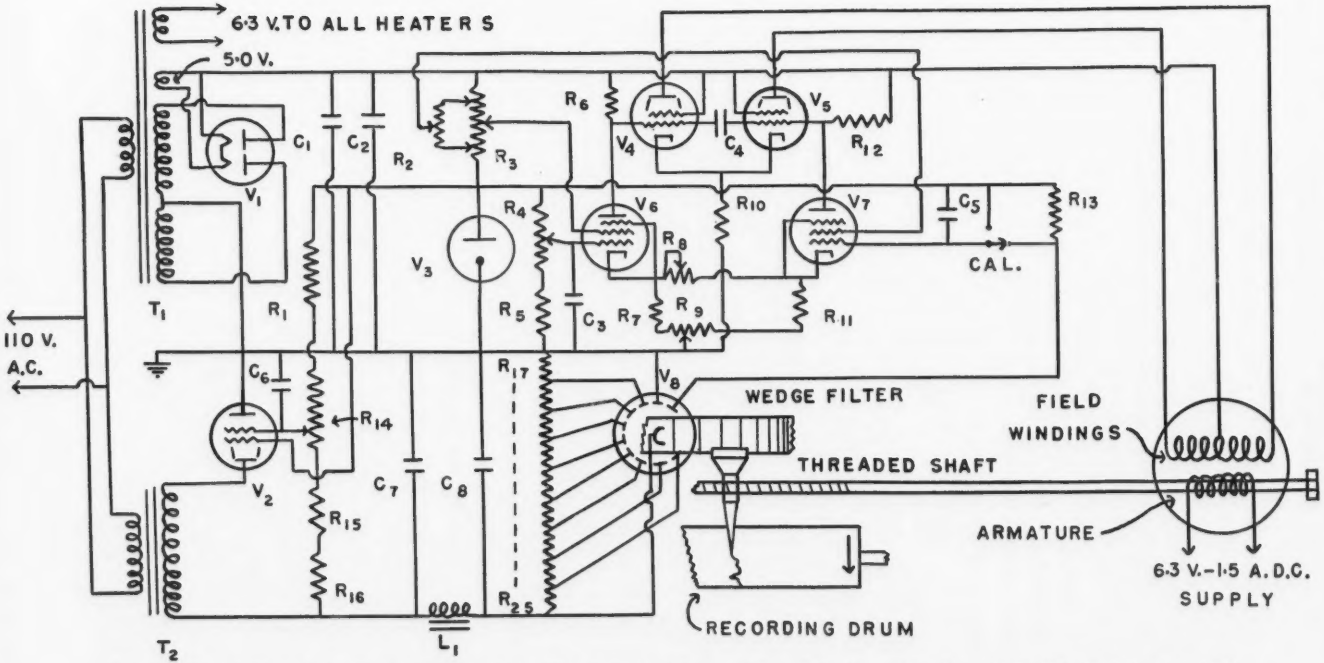

FIG. 1. *Circuit diagram for the auroral recorder. The electronic tubes are* V_1 *— 5R4;* V_2 *— 807;* V_3 *— V.R. 150;* V_4 *and* V_5 *— 6L6;* V_6 *and* V_7 *— 6SJ7; and* V_8 *— 1P21. The transformers are* T_1 *— 375-0-375 V; and* T_2 *— 0-1500 V. The resistances in ohms are* R_1 *and* R_4 *— 50,000;* R_2 *— 10,000;* R_3 *and* R_9 *— 25,000;* R_5 *— 220,000;* R_6 *and* R_8 *— 100,000;* R_7 *and* R_{11} *— 47,000;* R_{10} *— 2000, 25 watt;* R_{12} *and* R_{14} *— 100,000;* R_{13} *— 1 megohm;* R_{15} *and* R_{16} *— 300,000; and* R_{17} *to* R_{25} *— 47,000. The capacities of the condensers in microfarads are* C_1 *and* C_2 *— 40;* C_3, C_4 *and* C_5 *— 0.1;* C_6 *— 0.5; and* C_7 *and* C_8 *— 4. The inductance in henries is* L_1 *— 30.*

phototube, due to any low value of the light flux reaching the phototube, is balanced by the voltage drop across a variable resistor (R_4). These two voltages are applied to the grids of a balanced voltage amplifier (V_6 and V_7). The anodes of the tubes in the voltage amplifier are connected to the grids of a balanced power amplifier (V_4 and V_5). The currents from the tubes in the power amplifier flow in opposite directions through the split-field windings of a motor, so that the motor is motionless as long as the two currents are equal. A brass rod (53 threads per inch) is attached to the shaft of the motor, and carries a steel nut that is fastened to the filter. When the light flux reaching the phototube increases or decreases to a value where a voltage differential of about 0.25 v. from the preset condition is established, the motor rotates and moves the filter to a position that restores the initial balance.

A power supply (T_1 and V_1) delivers 120 ma. at 350 v. to the servo-mechanism, and also feeds a glow tube (V_3) through a resistor (R_3) to provide a + 150 v. source. This source provides the voltage drop across R_4 and R_5 that is used in balancing the voltage drop across R_{13}. It also provides the voltage for the final stage of the phototube. Small variations of the power supplied by this unit do not affect the operation of the recorder.

A second power supply (T_2 and V_2), consisting of a 1500 v. transformer and a beam power tetrode gives the adjustable and stabilized voltages that are required for the first nine stages of the phototube. The cathode of V_2 is grounded, and the end of the secondary winding of T_2 in series with the plate circuit is at an output voltage of -720 to -1080 v., depending on the setting of a rheostat (R_{14}). A potential divider (R_1, R_{14}, R_{15} and R_{16}) is connected between the output voltage and the aforementioned voltage of + 150 v. A portion of this potential difference (across R_{14}) is applied to the grid of V_2; and the positive side of the 150 v. supply is connected to the screen of V_2. If the output voltage changes, the portion of this change applied to the grid is of such a polarity as to cancel the variation in the output. This circuit gives a high degree of stabilization in the output voltage over a line voltage range of 83 to 135 v., a.c. The output voltage is applied to the dynodes of the phototube by means of a resistor chain (R_{17} to R_{25}), which is mounted on the base of the phototube.

The armature of the servo-motor operates on a current of about 1.5 amp. from a 6 v. supply. For convenience, a transformer giving a secondary voltage of about 6.3 v. and a copper oxide rectifier are used instead of a storage battery.

The wedge filter in use during the past year was made by exposing Process film in such a way that the resulting optical density across a 7 in. strip varied almost linearly from 0 to 3.5. However, suitable wedge filters having a somewhat larger density range are available commercially, and their purchase is recommended since a great number of trials is usually required before one with approximately linear characteristics can be made photographically.

The drum, which carries the paper past the pen, is driven by a small a-c. motor through a train of reducing gears so that the paper advances at the rate of about 4.5 in. per hr. A glazed paper (available commercially for recording galvanometers) about 11 in. wide is used. A satisfactory combination of pen and ink, for all weather conditions is still to be found. A satisfactory combination for active displays during cold weather gives a broad trace during periods of quiet aurora and warm weather. In addition to obscuring some of the finer detail in the auroral record, this broad trace smudges readily because of the time required for it to dry. So far, the nearest approach to a satisfactory pen is one made by drilling a hole of 0.013 in. diameter along the axis of a circular brass rod, bevelling the end of the rod with the hole until a tip about 0.03 in. diameter is formed, and then drilling out the other end to form an ink reservoir about 0.25 in. diameter. A fine wire of 0.012 in. diameter passes through the hole in the tip and rests on the paper when the pen is in use. The length of the hole partly determines the rate of flow of the ink. For the aforementioned dimensions a length of 0.25 in. gives the best results during warm weather. The type of ink that is used at the present time is one used for autographic meteorological instruments during cold weather.

Time marks are placed on the record at five-minute intervals by a second pen that is operated electromagnetically through the closing of a circuit by a master clock located in the laboratory. This clock is also used to start the recorder at a selected time each evening and to stop it the following morning.

Baffles with circular openings restrict the light flux to a cone with a half-angle of 22.5°. Ordinarily, the recorder is operated so that the axis of this cone passes through the zenith. A weatherproof box (28 by 19 by 23 in.) encloses the recorder, a circular glass plate in the top admitting the light flux.

Calibration marks are placed on the charts once each week by the unit that is shown diagrammatically in Fig. 2. This is placed over the window of the recorder. It excludes all light except that from a tungsten lamp that is operated at a known, constant voltage. A series of diffusing screens and diaphragms between the lamp and the recorder reduce the flux from the lamp to the same magnitude as that from the sky. A movable brass strip with a series of apertures of known diameters is used to admit different light fluxes to the phototube.

Experience with the Recorder

Experience with the recorder (intermittently during August and September, 1947, and almost continuously since then) indicates certain advantages and disadvantages of the recorder. With little or no moonlight or twilight and with clear skies, the duration of zenithal aurora per night can be determined with an estimated error of about five minutes, the time at which a rapid change of auroral intensity begins or ends can be determined to within 30 sec. of the actual time, and small changes of intensity that would certainly be ignored in visual observations are evident on the records. With increasing

moonlight or twilight, the durations of displays and the times at which large intensity changes occur become less certain, since the logarithmic response of the recorder gives a smaller displacement on the chart for an aurora of a given

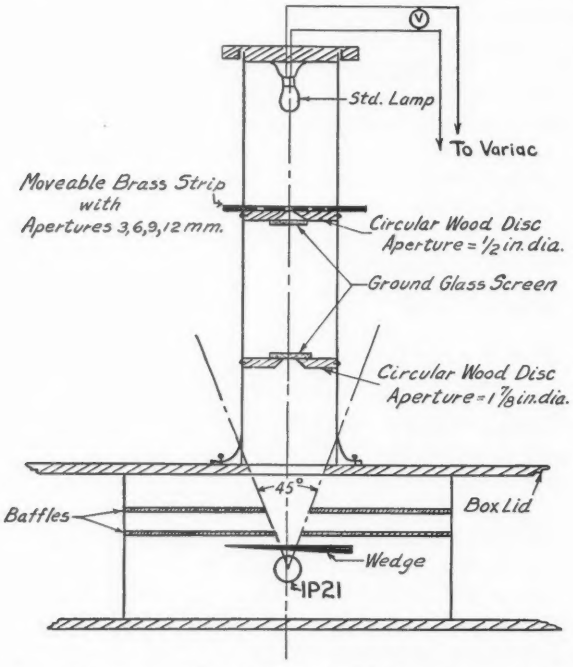

FIG. 2. *A semidiagrammatic sketch of the unit used for placing calibration marks on the charts of the auroral recorder.*

intensity when accompanied by moonlight or twilight than when the night is dark. However, the presence of all except faint aurora is evident as a superimposed variation on a regular trend in the trace due to the moonlight and twilight radiations. Broken cloud during periods of moonlight and twilight introduces an ambiguity into the record that cannot be settled with certainty. The direct effect of cloud is to reduce the recorded intensity. This can be readily detected by drawing a smooth curve on the chart for the intensity of the moonlight or twilight, if the sky had been clear. Unfortunately, light reaching the ground through breaks in the cloud cover is diffusively reflected back to the cloud and then to the recorder (especially with a snow cover), and gives a record that may be easily interpreted as one due to aurora. Reflection of the light from the city lamps by clouds also gives a record that is difficult to interpret.* Although the intensity of the aurora (in relative units)

* *It has been suggested that cloud in the zenithal sky could be registered on the record by using a small searchlight to flash a beam upward at periodic intervals.*

can be readily determined for any instant from the record, the average hourly intensity cannot be estimated as readily by inspection as on autographic records with a linear scale.

Figs. 3 and 4 show photographic reproductions of the auroral record for the night of March 14-15, 1948. This was a night with much quiet aurora in the zenithal sky, and with little cloud. The straight line that is drawn along the

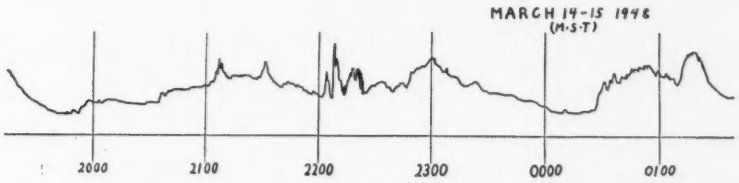

FIG. 3. *A photographic reproduction of the auroral record for the evening hours of March 14-15, 1948. The heavy, horizontal line near the bottom of the record indicates the intensity of the radiations from a clear sky without aurora.*

lower side of each record shows the position on the record corresponding to the light flux from the normal night sky. The upward trend in the record that starts at about 0400 hr. is due to the morning twilight. Superimposed on this part of the record is evidence of a very oscillatory type of aurora.

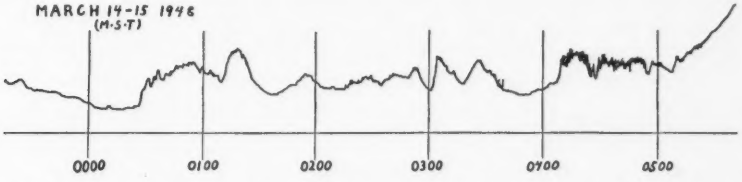

FIG. 4. *A photographic reproduction of the auroral record for the morning hours of March 14-15, 1948.*

Visual observations of aurora at Saskatoon indicate that this is a characteristic feature of aurora in this region just before sunrise. Pulses of auroral light travel in rapid succession upward to the zenith from the horizon toward the sun. While the time response of the recorder is too slow to record the full intensity of these pulses, it does indicate their occurrence. Some estimate of their intensity can be made by exposing the recorder to an intermittent source of illumination, and noting the frequency of illumination required to reduce the amplitude of the record to one-half of its value when the frequency of illumination is sufficiently slow for the maximum changes to be recorded.

Fig. 5 is a photographic reproduction of the auroral record for the night of May 14-15, 1948. The effects of twilight and some moonlight are evident in this record. The aurora on this occasion was more active than on March 14-15, probably owing to the presence of solar radiation in the upper atmosphere at this time of year.

Comparisons of the auroral records for four days of very active aurora at Saskatoon with the corresponding magnetic records from the Meanook Magnetic Observatory (54°37′N., 113°20′W.) showed remarkable similarities

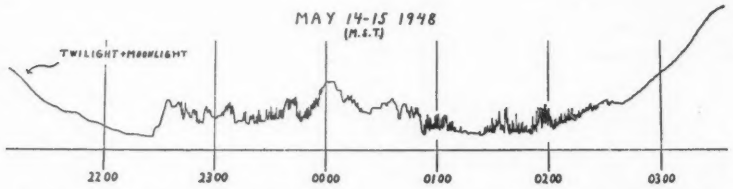

FIG. 5. *A photographic reproduction of the auroral record for the night of May 14-15, 1948.*

between the changes of auroral intensities and the variations of the *H* component and to a lesser extent of the *Z* component, although the two places are about 550 miles apart. However, both places have about the same geomagnetic latitude (61.8° N. for Meanook and 60.5° N. for Saskatoon), so that the changes in the current systems responsible for the magnetic variations at Meanook must have been accompanied by corresponding time variations of auroral intensity at Saskatoon. Again, the intensity changes during auroral displays on successive nights are occasionally so similar as to leave little doubt that some features of an aurora are repeated on successive nights. Still another feature of the records for the past year is the high frequency of aurora in the morning hours, indicating that the diurnal maximum at Saskatoon may occur three to four hours after local midnight.

A detailed analysis of the records will appear in a later communication.

Acknowledgment

The development of this recorder and its operation was made possible by financial assistance from the National Research Council of Canada.

References

1. GARTLEIN, C. W. Rochester Eng. 24 : 82. 1945.
2. GARTLEIN, C. W. Document T124, Eighth Assembly, International Union of Geodesy and Geophysics. Oslo. 1948.
3. HARANG, L. Terr. Magn. Atm. Elec. 37 : 167. 1932.
4. HARANG, L. Terr. Magn. Atm. Elec. 51 : 353. 1946.
5. SWEET, M. H. J. Optical Soc. Am. 37 : 432. 1947.
6. VEGARD, L. Section on the aurora *in* Terrestrial magnetism and atmospheric electricity. *Edited by* J. A. Fleming. McGraw-Hill Book Company, Inc., New York. 1939.

DETERMINATION OF THE ELEMENTS OF METEOR PATHS FROM RADAR OBSERVATIONS[1]

By D. W. R. McKinley and Peter M. Millman

Abstract

Methods of determining meteor velocities from single-station observations are discussed. Where three-station observations are available both the velocity and the elements of the meteor's path through the atmosphere can be computed in favorable cases. These methods are applied to a selected daytime meteor, recorded by the three radar stations at $17^h\ 59^m\ 48^s$ E.S.T., Aug. 4, 1948. The following elements of the meteor's path have been obtained from the radar data;—

Apparent geocentric velocity	35.0 ± 0.4 km. per sec.
True bearing of apparent radiant	$074° \pm 2°$
Elevation of apparent radiant	$2° \pm 2°$
Total radar path length	270 km.
Height above sea level	108—104 km.

These values lead to an orbit similar to one of the short-period comets, with these elements:—

Semi-major axis	a	2.66
Eccentricity	e	0.87
Angle node to perihelion	ω	294°9
Longitude of node	Ω	132°4
Inclination	i	33°6
Period	P	4.33 years

Introduction

It is now well established that the ionization produced by the passage of a meteor through the atmosphere at heights in the neighborhood of 100 km. above the earth can be detected by conventional radar equipment operating in the frequency range 3 to 200 Mc. per second. Assuming that the other parameters of the radar system remain constant it has been found that the meteor echo rates vary roughly as the square of the wave length. The durations of the echoes exhibit a similar dependence on the wave length. At first glance it would seem that the longer the wave length the better for the radar observation of meteors but several factors must be taken into consideration. If steerable directive antennas are to be used the shorter wave lengths are obviously preferable because the physical size of an array of given gain may be reasonable at 4 meters, say, but prohibitive at 40 meters. On the shorter wave lengths the echo is usually received only from a short portion of the meteor path in the immediate vicinity of the point where the meteor crosses the line of sight at right angles (17). This normal reflection law has been used by Hey and Stewart (5), Clegg (1), and McKinley and Millman (7) to determine the radiants of meteor showers by various techniques. On the

[1] *Manuscript received January 27, 1949.*

Contribution from the Radio and Electrical Engineering Division, National Research Laboratories, and from the Dominion Observatory, Ottawa, Canada. Issued as N.R.C. No. 1927, and Contributions from the Dominion Observatory, Vol. II, No. 5.

longer wave lengths a longer portion of the meteor path becomes visible on the radar display, subject to the limitation that detectable ionization is usually produced only within the *M*-region (7) extending from 80 km. to 110 km. above sea level. Another point worthy of consideration in the choice of an operating wave length is the interference to be encountered on the longer wave lengths from distant high-frequency transmitting stations. Daytime absorption of the radio wave in the upper atmosphere is more pronounced on the longer wave lengths.

Taking all these factors into account it was decided to use radio frequencies in the band 30 to 36 Mc. per second (10.0 to 8.3 meters) as a reasonable compromise. Three complete and independent radar stations were installed, at Ottawa, Arnprior, and Carleton Place, see Fig. 1. The Ottawa station

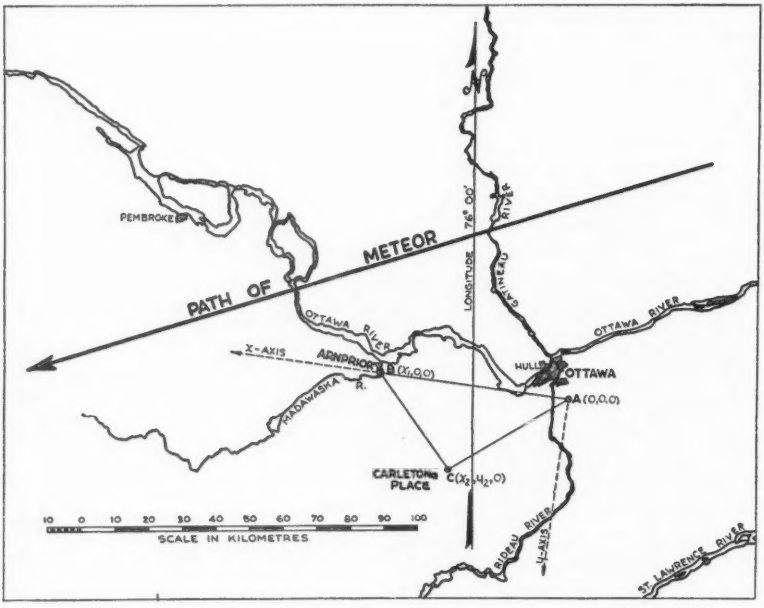

FIG. 1. *Map showing positions of radar stations and path of meteor at 17h 59m 48s E.S.T. Aug. 4th, 1948.*

has been operated intermittently since August, 1947, and the Arnprior station was first put on the air in April, 1948. The Carleton Place station commenced operation about the first of August, 1948, and all three stations were run on a 24 hr. schedule for the annual Perseid shower during the first two weeks of August. The geographical co-ordinates, base lines between the three stations, and the essential electrical parameters are given in Table I.

TABLE I

	A-Ottawa	*B*-Arnprior	*C*-Carleton Place
Latitude N	45° 20′ 32″	45° 24′ 55″	45° 09′ 20″
Longitude W	75° 36′ 05″	76° 21′ 38″	76° 05′ 17″
Interstation distances, km.	$AB = 57.44$	$BC = 35.94$	$CA = 41.20$
Transmitter peak power, kw.	400	50	50
Pulse width, μsec.	20	8	8
Receiver sensitivity, w.	2×10^{-14}	5×10^{-14}	5×10^{-14}
Radio-frequency, Mc./sec.	32.7	36.0	34.5
Antennas	Half-wave horizontal dipoles, mounted a quarter-wave above ground		
	Orientation N-S	Orientation NW-SE	Orientation NW-SE
Display	Range-time sweep, intensity-modulated by signal		

The range-time display is similar to the one conventionally used in ionospheric recording. A horizontal linear sweep, about 350 km. long, is displayed on a 5GP11 cathode ray tube. Twenty-kilometer negative marker pips are applied to the intensity-grid of the c.r.t. for range calibration. Seconds pulses received by radio at the three locations from station CHU operated by the Time Services of the Dominion Observatory (19) are fed through special circuits which produce positive pips on the intensity grid. These seconds pips are applied twice to the range sweep, near minimum and also near maximum range, so that alignment errors in the recording system can be eliminated. A special camera photographs the range sweep continuously on a 100 ft. roll of 35 mm. film which is moved at a constant speed past the open lens. Film speeds of $\frac{1}{2}$, $\frac{3}{4}$, 1, 2, and 4 in. per min. are available. The positive video output from the receiver is passed through a limiter circuit and applied to the intensity-grid of the cathode-ray tube.

Suppose that a target moving through space in a straight line with a constant velocity v is detected by the radar system. The echo on the range-time display will describe a hyperbola, defined by:

$$R^2 = R_0^2 + v^2 (t - t_0)^2, \tag{1}$$

where R is the range to the target at time t and R_0 is the minimum range to the straight line path of the target at time t_0. In general, a meteor will produce detectable ionization only while traveling between the approximate height levels of 110 and 80 km., so that the possible ionized path length will depend on the inclination of the meteor's path to the tangent plane of the earth—that is, on the angle of elevation of the meteor radiant. A bright meteor traveling nearly tangentially to the earth's surface could thus produce an ionized path several hundred kilometers long, but a similar meteor arriving

from near the zenith would produce ionization over 10 to 30 km. only of its path. Whether or not all or a part of this ionized path is actually detected by the radar system depends on a number of conditions. A faint meteor can usually be detected only over a very short path length in the neighborhood of the R_0 point, and if this point on the path does not fall within the M-region no echo is seen. A bright meteor can be detected over a longer portion of its ionized path, even if this portion is located on the hyperbola at some distance from the R_0 point, on either the approaching or the receding branch. The picture is further complicated in many cases by the appearance of echoes definitely associated with the meteor, but delayed in time after the passage of the meteor. The various characteristic echoes and a theory to account for them are discussed in detail elsewhere, and a classification table (7, 9) has been drawn up to aid in describing the echo types seen on the range-time display. In this paper we shall consider only those echoes which appear to have a clearly defined component (*h* characteristic) moving with the meteor velocity. In the terminology of the classification table these will be the *Ah*, *Dh*, or *Uh* types, and the more complicated examples of these types, such as an *Ahbe3* echo. Echoes falling in the *Ab*, *Db*, or *Ub* classes are not as reliable for velocity determination, as experience has shown that the leading-edge envelope of the echo curve on the range-time display often yields an equivalent velocity somewhat lower than the real velocity of the meteor. *Af*, *Ae*, *Df*, and *De* echoes are quite useless for meteor velocity determinations because the apparent velocity they exhibit is not directly related to the actual meteor velocity, but depends on rather complicated factors involving wind drifts and possible changes of the reflection points on the trail (5), rates of expansion and decay of the ionized cloud, and delays in the appearance of the echo from various parts of the trail. These delays are functions of the height of the trail and of the angle between the meteor path and the observer.

Determination of Meteor Velocities from Single-station Observations

The first determination of meteor velocities from radar data was made by Hey, Parsons, and Stewart (4) using their observations on 60 Mc. during the Giacobinid shower in 1946. They obtained a faint fast-moving echo (*h* characteristic in our classification) which was assumed to have the meteoric velocity. From 22 tracks a velocity of 22.9 ± 1.3 km. per sec. was found and this corresponded satisfactorily with the theoretical velocity of 23.7 km. per sec. as computed from the cometary orbit. The *h* characteristic echoes detected on the lower frequencies used in our work appear more frequently and extend over a considerably greater path length than those observed by Hey, Parsons, and Stewart. On this basis the potential accuracy of our velocity measurements might be expected to be better. Other factors enter the problem, of course, and will be considered later.

To illustrate the discussion, let us refer to Fig. 2, which shows a meteor echo that appeared as type *Uhb* at all three stations on Aug. 4, 1948, at $17^h\ 59^m\ 45\text{–}53^s$ E.S.T. As this meteor occurred during daylight no visual

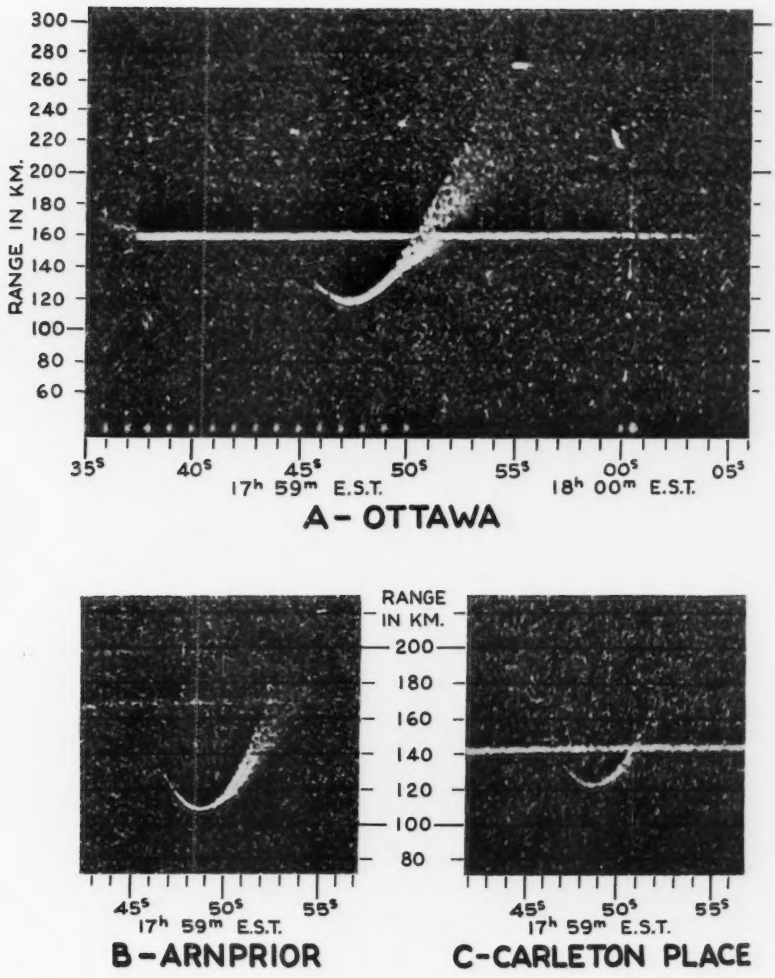

FIG. 2. *Meteor echoes photographed at the three stations on Aug. 4th, 1948:—*

(a) A Uhb echo at 17h 59m 45-53s. This is the echo that is considered in detail in this paper.

(b) An F echo at 17h 59m 37s, enduring for 27 sec. on the Ottawa record. This echo first appeared at a true height of 101 km. with bearing 197° and ground distance 120 km. from Ottawa. After 15 sec. the height of the echo was 94 km. and the apparent drift of the echo was about 20 km. in a southeast direction.

(c) Visible on the Ottawa photograph are an F echo at 17h 59m 55s, range 270 km., duration one second, and an Ah echo at 17h 59m 59s, range 228 to 216 km. As these echoes did not appear at the other stations it was not possible to triangulate heights and positions.

or photographic observations were available. Various techniques for measuring the velocity of such an echo have been evolved and four of these methods are described below.

(i) *Curve-fitting Method*

It is possible to fit hyperbolic curves directly to an enlargement of any one of the *Uhb* echoes of Fig. 2 and thus to determine by trial and error the best fit. This will give only an approximate value of the velocity because the range-time record suffers from several small distortions. For example, the range sweep is slightly nonlinear, so that the spacing of the 20-km. pips is not quite uniform; the sweep may have a slight bend due to stray steady magnetic fields; and the range axis may not be truly orthogonal to the time axis because of errors in lining up the c.r.t.-camera system. These irregularities can be eliminated by transferring the original echo curve point by point to a large sheet of standard graph paper. To do this the range intervals are first measured and then plotted to determine the range correction factor to be applied at any given range of the echo curve. Next, the time intervals are similarly measured and any necessary correction factors applied, though the time intervals are usually quite uniform. Any curvature in the c.r.t. sweep can be detected by momentarily brightening the sweep from time to time during the observations. This curved R axis must be used in reading points from the original photograph. Having transferred the echo curve to Cartesian co-ordinate paper, it becomes a simple matter to calculate and plot hyperbolae with the observational values of R_0 and t_0 and with various assumed values of v until the best fit is obtained with the observational curve. Probable upper and lower limits of velocity can be assigned by drawing curves which bracket the points of the observational curve. It may happen that the original curve deviates from a true hyperbola by more than the observational and measurement errors. When this occurs it is usually possible to explain the deviation in terms of the time delays associated with the angle of elongation of the meteor and height within the M-region, and small empirical corrections, deduced from known cases, can be applied with fair success.

(ii) $R\dot{R}$ *Method*

In many cases of the *Ah* and *Dh* echo types, the echo segment of the hyperbola does not include the R_0, t_0 point, so that the simple curve-fitting technique described above is difficult to apply. If the segment is long enough and sufficiently well delineated to allow the curvature to be accurately measured, it is possible to calculate the velocity, and at the same time to determine the R_0, t_0 points with fair precision. Differentiating Equation (1) with respect to time, we have:

$$R\dot{R} = v^2t - v^2t_0 \,, \tag{2}$$

so that if $R\dot{R}$ is plotted against t we should obtain a straight line with slope v^2. The values of $\dot{R}$ may be obtained by precision measurements of the slope of the observational curve at selected points, either by graphical methods or by calculating differences. The time at which the line crosses the t-axis is the t_0 point. It is easier to fit a straight line to a set of points which are presumed to satisfy a linear relation than it is to fit a curve to the same observational data in hyperbolic form. In practice, the least squares method of determining the best straight line is used. Estimates are also made of probable error in v^2 due to the observational scatter, probable errors in measurement and reduction of the photograph, and probable errors in the range and time calibration.

(iii) *Three-Point Method*

Another method for the evaluation of v^2 involves substituting in Equation (1) three R, t values obtained from widely different parts of the observational curve, and solving the three equations simultaneously for v^2. The algebra is straight-forward and yields for v^2 the formula:

$$v^2 = \frac{R_1^2 (t_3 - t_2) - R_2^2 (t_3 - t_1) + R_3^2 (t_2 - t_1)}{(t_2 - t_1)(t_3 - t_2)(t_3 - t_1)} . \qquad (3)$$

Uniform time intervals are usually selected so that this expression becomes simplified for practical computations. Needless to say, several sets of three-point values are used in calculating a mean v^2. The t_0 point can also be computed from a similar formula.

(iv) *Parabolic Regression Method*

The curvilinear regression method of least squares (6) was also used in computing v. For this purpose ρ is written for R^2 in Equation (1) so that a parabolic relation should obtain between the observed values of ρ and t. The usual sets of normal equations are written down and solved. This method does use all the observational data simultaneously, but the calculations are rather tedious, and do not appear to lead to an answer that is any more trustworthy than that obtained by Methods (ii) or (iii).

The three types of errors that can affect the velocity determination are, in increasing order of importance, the basic errors in the range and time calibrations, the errors in measurement and reduction of the films, and the errors introduced by factors not under the control of the observer, such as the delays in echo appearance, and signal strength fluctuations.

The average timing error between consecutive seconds pulses is of the order of 0.02 sec. However, these pulses are supplied from a source with an integrated accuracy of 1 part in 10^6 or better so that if a number of seconds intervals are measured on the film, the basic error in timing can be reduced to the order of 0.001 sec., which is insignificant in the analysis. The intrinsic

accuracy of the 20 km. range markers is at present of the order of 0.1 km. over the working range of the display, and could be further improved if required. The effect of this range error on the single-station determination of v depends both on the value of v and on the mean range interval over which the echo is observed, but rarely contributes more than 0.1% to the error in v.

The sources of errors in measurement and reduction of the film have been discussed to some extent above. Careful application of all the scale correction factors involved is required to transfer the echo curve to large-scale co-ordinate paper. An inexperienced worker may introduce errors which affect the velocity by as much as 1 or 2%, but, with a skilled analyst, the reduction errors introduced at this stage are not significant in comparison with the larger errors to be considered below.

The greatest source of error lies in determining the real outline of the echo hyperbola—that is, in drawing on the photograph the thin line on which the measurements are made. The pulse width, the pulse rise time, the echo signal strength, and the probable delay times in the appearance of the echo at various parts of the path all have to be taken into consideration. When considering an *Ah* echo, the pulse width is immaterial, but the pulse rise time can cause small variations of the order of 0.3 km. in the apparent range measurements if the signal strength varies from barely detectable to saturation level. The density and width of the echo furnish a good indication of the signal strength up to the clipping level of the video limiter, and for higher signal strengths the length of the black shadow, due to the video overshoot, is a measure of signal strength. With these considerations in mind, a line can be drawn at or near the lower edge of the *Ah* echo. The *Dh* echoes are sometimes more difficult to treat. If the *Dh* echo is clean, i.e., with no trailing enduring part, the same technique is used as for the *Ah* types. More usually the *Dh* type has a reasonably well defined upper edge and a diffuse lower edge (*b* characteristic) so that the lower edge cannot be used. In these cases, the upper edge is used as the reference and the curve is drawn through points obtained by subtracting small distance intervals which are equal to or less than the pulse width in kilometers, depending on the signal strength and other factors mentioned above. In general, a *Dh* echo does not yield as reliable a velocity determination as the *Ah* or *Uh* types.

Determination of Meteor Paths from Three-station Observations

It will be apparent that in computing the meteor velocity from a range-time photograph made at a single station, the t_0 point is of little interest, except in the curve-fitting method. However, when computing the meteor path by triangulation from photographs made at three stations, it is essential to determine the three t_0 points with the greatest possible accuracy. The probable error of t_0 in Method (i) is of the order of 0.2 sec. or greater and the technique is applicable only to the *Uh* types. The probable error of t_0 in Methods (ii), (iii), and (iv) is of the order of 0.01 to 0.05 sec. when dealing with the *Uh* types, and of the order of 0.05 to 0.2 sec. in the *Ah* and *Dh*

cases, depending on the length and definition of the echo from the observed segment of the path. Accordingly, one or more of the latter three methods is used to determine the t_0's at stations A, B, and C. The independent velocity determinations made at the three stations should agree within the respective probable errors, of course, and the data from all three stations are used in reaching a final weighted mean value of v. From Equation (1), using v and the t_0 values, the R_0 points at the three stations can now be calculated with considerably greater precision than is afforded by an inspection of the observational curves.

In computing the meteor path in space it is convenient to adopt Cartesian co-ordinates with the Ottawa station (A) at the origin, the Arnprior station (B) on the x-axis at (x_1, o, o) and the Carleton Place station (C) at the point (x_2, y_2, o) in the x, y-plane through the three stations (see Fig. 1). If, at any given instant, the range of a target from Station A is R_A, from Station B is R_B, and from Station C is R_C, then the position of the target (x, y, z) is defined by the intersection of the spheres:

$$x^2 + y^2 + z^2 = R_A^2 \tag{4}$$

$$(x - x_1)^2 + y^2 + z^2 = R_B^2 \tag{5}$$

$$(x - x_2)^2 + (y - y_2)^2 + z^2 = R_C^2 \tag{6}$$

whence,

$$x = \frac{R_A^2 - R_B^2 + x_1^2}{2x_1} \tag{7}$$

$$y = \frac{R_A^2 - R_C^2 + x_2^2 + y_2^2}{2y_2} - x\frac{x_2}{y_2} \tag{8}$$

$$z = (R_A^2 - x^2 - y^2)^{\frac{1}{2}} . \tag{9}$$

By inserting various simultaneous values of R_A, R_B, and R_C, each set of values being measured from the three observational curves at a selected instant in time, one can plot the meteor path in space. The points so obtained tend to be somewhat scattered because of small uncertainties in the determination of absolute time at the three stations. With present techniques these uncertainties are of the order of a few hundredths of a second.

A more satisfactory result can be achieved by using the data available from the velocity computations; namely, the mean value of v, the minimum ranges at the three stations, R_{0A}, R_{0B}, R_{0C}, and the corresponding times, t_{0A}, t_{0B}, t_{0C}. Equation (1) is then used to compute values of R_A, R_B, R_C at selected times. These sets of values are then inserted in Equations (7), (8), and (9), and a space plot of the meteor path is obtained. It can be shown that the x and y values computed in this particular manner will each be a linear function of time so that the horizontal projection of the path will be a straight line. This line will represent the best straight line that can be drawn through the x, y points that were obtained by direct triangulation. Owing to the arbitrary

sequence of Equations (7), (8), and (9) there will be a second-degree relation between z and t in general, though if the data were perfect the relation would become linear. In practice there will usually be a slight curvature of the computed path in the vertical plane, this curvature being attributable to small errors in v, R_{0A}, R_{0B}, R_{0C}, t_{0A}, t_{0B}, t_{0C}. It is possible to make small empirical adjustments to these parameters which will straighten out the space plot, but care should be taken that each correction is smaller than the probable error of the respective parameter. Because of the small intervals between the t_0 points the uncertainties in determining absolute time at the three stations tend to be more important than the errors in the other variables, so that any necessary adjustments are usually made to the t_0 parameters. However, this correction process should not be carried beyond the limitations of the observational data, as the effect on the orientation of the meteor path is not significant.

In practice the x and y co-ordinates are plotted on the ground plane map to show the projection of the meteor path, but the z co-ordinate is more conveniently plotted separately against time. The azimuth angle of the meteor path can be read directly from the map, and the elevation angle may be easily calculated from the z, t plot by making use of the velocity.

In the above discussion it has been assumed that the meteor path is theoretically a straight line. In general, the deviation of the observed path from a straight line owing to the earth's gravity (zenith attraction) and the rotation of the earth (diurnal aberration) will be measured in fractions of a degree, and is too small to be significant with the accuracy of measurement at present available. Where appreciable deceleration occurs, the meteor path will deviate from a straight line in the vertical plane but not in the x, y plane. Irregularities in the meteor path, such as those caused by explosions or bursts, may produce small deviations from linearity. Whipple (20) finds these are only very rarely as great as a third of a degree.

It might be remarked that meteor velocities can also be obtained by using a continuous-wave transmitter and measuring the Doppler whistles produced by the meteor echo (8). We have recently used this method, which yields accurate velocities from much shorter path lengths than those required for the radar method. We feel that a combination of techniques, using Doppler whistles for the velocities and three-station radar triangulation for the path positions, may greatly increase the number of meteors available for detailed path computations.

The Computation of a Meteor Path and Orbit

The *Uhb* meteor echo at $17^h\ 59^m\ 48^s$ Aug. 4th, 1948, shown in Fig. 2, is remarkable in the length of path visible by radar, and is a type rarely oberved. During 2000 hr. of observations, about 50 such echoes displaying an ionized path well over 100 km. long have been photographed, and of this number only a dozen or so were obtained while all three stations were operating.

The reason for their rare occurrence is that the meteor must be traveling at a low angle to the horizontal plane and should be of a mass sufficient to ensure that it will not be completely vaporized for several seconds. The probability of a sporadic meteor which satisfies both these conditions occurring within range of the radar stations is very small. A strong meteor shower should increase the chances at the times of rising and setting of the shower radiant. Two striking photographs (9) of Lyrid meteor echoes were obtained on April 21, 1948, when the radiant was very low in the sky, though unfortunately only one station was operating at the time. The summer daytime showers (2), extending through May, June, and July also produced several such echoes, particularly when the radiants were setting. Several hundred meteor echo photographs are available which show from 50 to 100 km. path length, produced by meteors with higher radiants. The elements of the meteor paths calculated from these photographs have probable errors two or three times greater than the errors assigned to the exceptional low-angle cases.

As the preceding sections may have indicated, the work of reducing a three-station meteor echo is somewhat tedious and, therefore, will not be reproduced in detail. In the present case all four of the methods for measuring velocity were applied to the photographs and each yielded a velocity measurement agreeing with the others within the limits of the errors. The data for the $R\dot{R}$ method, for example, are plotted in Fig. 3 to show the dispersion of the points about the straight lines. The highest points on the Ottawa and Arnprior plots tend to show an upward curvature, and these are omitted in calculating the least squares lines, because they are derived from the less reliable parts of the original hyperbolae. The t_0 times for the three stations can be read immediately from Fig. 3 to an accuracy of the order of 0.03 second.

The smoothed path of the meteor was computed from the mean value of v and the R_0 and t_0 values, and it was noted that the horizontal projection of this path agreed well with the x, y points obtained by direct triangulation, the average deviation of the points being less than 2 km. Some apparent curvature in the z, t plot was reduced slightly by making small corrections to the t_0 times. The effect of this procedure on the horizontal plot was negligible. The x, y plot of the meteor path is shown in Fig. 1, and the z, t plot in Fig. 4. The solid portion of the straight line drawn through the points of Fig. 4 indicates the 160 km. of path length that was observed in common at all three stations, and the dotted extensions show the total path length as observed at the Ottawa station only. The apparent precision of the line in Fig. 4 is somewhat misleading, as the points are computed from smoothed data. The elevation of the radiant as deduced from this line is $+ 1°$ but it would be safer to assume a mean elevation of $+ 2°$ with a probable error of 2°, though this may be unnecessarily conservative. Entirely apart from the measurements made above it is possible to assign an upper limit of about 4° for the elevation solely on the assumption that the meteor fell 20 km. (the average effective thickness of the M-region) in its total recorded path length of 270 km.

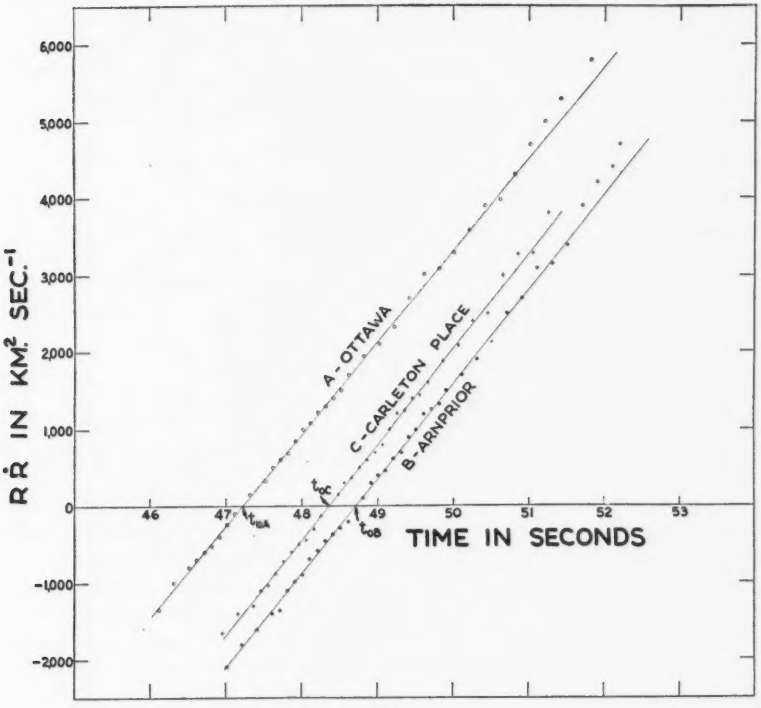

FIG. 3.

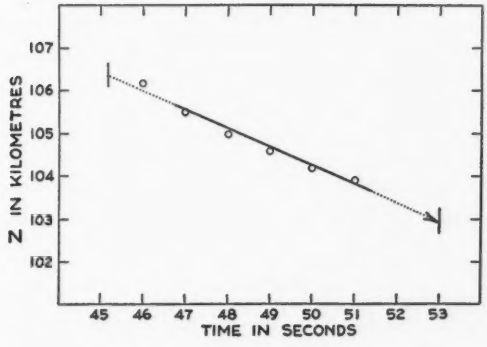

FIG. 4.

The radar data for this meteor are summarized in Table II.

It should be noted that the z values in Fig. 4 refer to heights above the co-ordinate plane through the three stations. True heights above sea level

TABLE II

	A-Ottawa	*B*-Arnprior	*C*-Carleton Place
R_0, km.	117.8	108.6	122.1
t_0, sec.	47.22	48.71	48.36
v, km./sec.	34.7 ± 0.6	35.3 ± 0.6	35.1 ± 0.6
Observed path length, km.	270	175	160

Apparent geocentric velocity	35.0 ± 0.4 km. per sec.
Apparent radiant—true bearing	074° ± 2°
—elevation	+2° ± 2°
True height above sea level—beginning of path	108 km.
—end of path	104 km.

are obtained by correcting these values for the effects of the earth's curvature and the altitudes of the three stations. The height figures given in Table II refer to the beginning and end of the 270 km. path length observed at Ottawa.

The position of the apparent radiant determined above, when corrected for zenith attraction and diurnal aberration, gives a corrected radiant just one degree below the horizon at R.A. 324°.7, Dec. + 10°.6. This radiant position is within two degrees of the star ϵ Pegasi. An examination, by no means exhaustive, of various radiant lists (3, 10–16, 18) reveals nothing very striking in this region for the first week of August. Most of the radiants in this part of the sky are associated with the δ Aquarid shower and are located south of the equator rather than north. Radiant group No. 250 of Denning, radiants Nos. 1118, 1130, 1134, 1622, and 2225 of the American Meteor Society, and radiant No. 131 published by the Russian observers in Mïrovédénïé, 1925, are near ϵ Pegasi. These are all weak radiants represented by only four to seven meteors each. The meteor discussed in this paper may hence be considered to belong to the type generally classed as sporadic.

For the computation of the orbit about the sun it seemed advisable to take two possible positions of the apparent radiant, one at the observed elevation of 2° above the horizon, giving the meteor orbit, and the other at the maximum elevation that could be considered consistent with the radar data, i.e., 4° above the horizon. This second radiant position provides an alternative orbit which gives an indication of the order of magnitude of the changes in the elements resulting from a shift of the apparent radiant by two degrees. The computation of the two orbits was carried out by the Laplacian method, making use of the convenient summary of formulae published by Wylie (21).

The heliocentric velocity of the meteor was 37.6 km. per sec., well below the parabolic velocity for this date, 41.8 km. per sec. Both computed orbits are ellipses with eccentricities of 0.87 and aphelion points about the same distance from the sun as Jupiter's orbit. These orbits are therefore similar

to those of the short-period comets of Jupiter's family (22) but with somewhat higher eccentricities. The inclinations are near the upper limit for short-period meteor orbits determined up to the present. The orbital elements, for the equinox of date, are listed in Table III. The semi-major axes are given in

TABLE III

		Meteor orbit	Alternative orbit
Semi-major axis	a	2.66	2.98
Eccentricity	e	0.868	0.872
Angle node to perihelion	ω	294°9	290°8
Node	Ω	132°4	132°4
Inclination	i	33°6	34°8
Period, years	P	4.33	5.15

terms of the earth's mean distance from the sun. These orbits have been plotted in Fig. 5.

The changes in the elements resulting from the probable error in the observed velocity are, on the whole, smaller than those due to the uncertainties of radiant position. For example, if the observed velocity is assumed to be 34.6 km. per sec. we have $a = 2.49$, $e = 0.858$, $\omega = 294°6$, $i = 33°3$ and $P = 3.92$ years, giving an ellipse somewhat smaller than the plotted meteor orbit. The correction to the observed velocity for diurnal aberration was -0.3 km. per sec. for this meteor. This is less than the probable error in the observed velocity and was not included in the orbit computation.

The techniques here illustrated are applicable to individual echoes and hence should be particularly useful in examining specific meteors, either by day or by night, with a view to determining whether their orbits are hyperbolic or elliptical. This is an important consideration in any theory of the origin of meteors. While we have not yet made a detailed statistical study of meteor velocities it may be remarked that there has been no indication up to the present of hyperbolic orbits in the radar and Doppler data which we have accumulated.

Acknowledgments

It is a pleasure to record that three summer assistants, Dr. H. Kaufman, Mr. H. D. Griffiths, and Mr. R. L. Stauffer, carried out most of the computations of meteor velocity and three-station triangulation upon which this paper is based. Mr. E. L. R. Webb, with Mr. R. S. McClean as his assistant, supervised the design, construction, and operation of the radar equipment, while Mr. B. E. Bourne was responsible for many of the circuit details. It

would not have been possible to maintain the three radar stations on a 24 hr. watch for two weeks in August, 1948, without the enthusiastic co-operation of all personnel connected with the project.

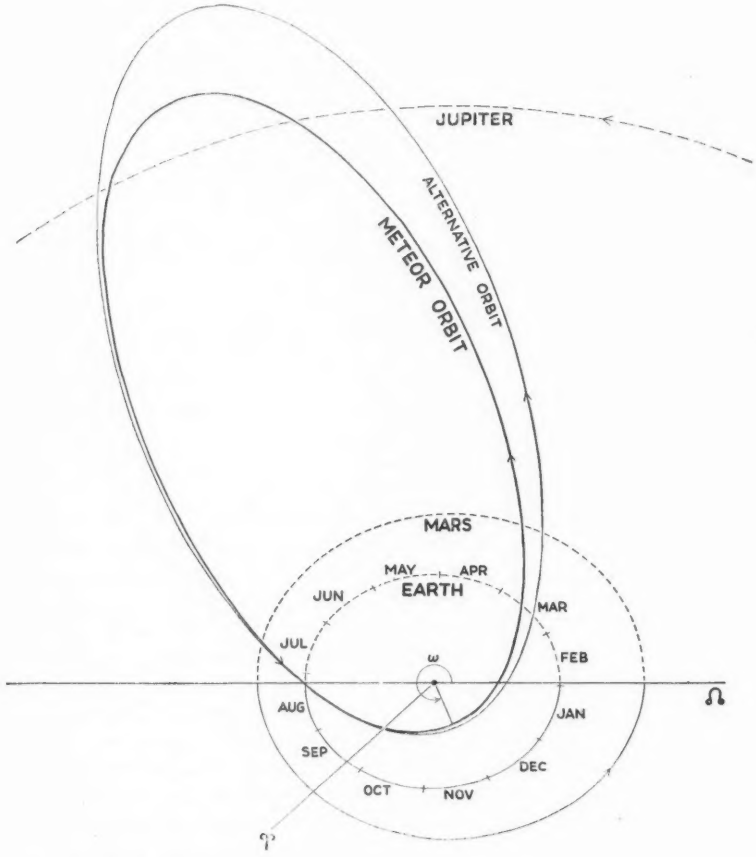

FIG. 5. *Computed meteor orbit.*

The Meteor Orbit, apparent radiant elevation + 2°, and the Alternative Orbit, apparent radiant elevation + 4°, have been plotted in the plane of the paper. The planetary orbits, inclined by approximately 34° to this plane, have been projected on to it.

References

1. CLEGG, J. A. Phil. Mag. (Ser. 7) 39 : 577. 1948.
2. CLEGG, J. A., HUGHES, V. A., and LOVELL, A. C. B. Monthly Notices Roy. Astron. Soc. 107: 369. 1947.
3. DENNING, W. F. Mem. Roy. Astron. Soc. 53: 203. 1899.

4. HEY, J. S., PARSONS, S. J., and STEWART, G. S. Monthly Notices Roy. Astron. Soc. 107: 176. 1947.
5. HEY, J. S. and STEWART, G. S. Proc. Phys. Soc. (London), 59: 858. 1947.
6. HOEL, P. G. Introduction to mathematical statistics, pp. 89-90, 130-132, and 147-150. John Wiley & Sons, Inc., New York. 1947.
7. McKINLEY, D. W. R. and MILLMAN, PETER M. Proc. Inst. Radio Engrs. 37 : 364. 1949.
8. MANNING, L. A. J. Applied Phys. 19: 689. 1948.
9. MILLMAN, PETER M. and McKINLEY, D. W. R. J. Roy. Astron. Soc. Can. 42 : 121. 1948.
10 ÖPIK, ERNST. Harvard Coll. Observ. Circ. No. 388. 1934.
11. OLIVIER, C. P. Trans. Am. Phil. Soc. 22: 5. 1911.
12. OLIVIER, C. P. Pub. Leander McCormick Observ. 2: 131. 1914.
13. OLIVIER, C. P. Pub. Leander McCormick Observ. 2: 199. 1921.
14. OLIVIER, C. P. Pub. Leander McCormick Observ. 5: 1. 1929.
15. OLIVIER, C. P. Popular Astron. Meteor Notes, 1928-1947.
16. POKROVSKY, K. Pub. Tartu Observ. 25, No. 4: 77. 1923.
17. PRENTICE, J. P. M., LOVELL, A. C. B., and BANWELL, C. F. Monthly Notices Roy. Astron. Soc. 107: 155. 1947.
18. RUSSIAN AMATEUR SOCIETY FOR THE STUDY OF THE UNIVERSE, LENINGRAD, U.S.S.R., Section for the Observation of Meteors. Mirovédénié, Astronomical Bulletin. 1925-1930.
19. THOMSON, M. M. J. Roy. Astron. Soc. Can. 42: 105. 1948.
20. WHIPPLE, FRED L. Proc. Am. Phil. Soc. 91 : 189. 1947.
21. WYLIE, C. C. Popular Astron. 47: 425. 1939.
22. YAMAMOTO, A. S. Preliminary general catalogue of comets. Pub. Kwasan Observ. 1: No. 4. 1936.

CANADIAN JOURNAL OF RESEARCH

Notes on the Preparation of Copy

GENERAL:—Manuscripts should be typewritten, double spaced, and the **original and one extra copy** submitted. Style, arrangement, spelling, and abbreviations should conform to the usage of this Journal. Names of all simple compounds, rather than their formulae, should be used in the text. Greek letters or unusual signs should be written plainly or explained by marginal notes. Superscripts and subscripts must be legible and carefully placed. Manuscripts should be carefully checked before being submitted, to reduce the need for changes after the type has been set. If authors require changes to be made after the type is set, they will be charged for changes that are considered to be excessive. **All pages, whether text, figures, or tables, should be numbered.**

ABSTRACT:—**An abstract of not more than about 200 words, indicating the scope of the work and the principal findings, is required.**

ILLUSTRATIONS:

(i) *Line Drawings:*—All lines should be of sufficient thickness to reproduce well. Drawings should be carefully made with India ink on white drawing paper, blue tracing linen, or co-ordinate paper **ruled in blue only;** any co-ordinate lines that are to appear in the reproduction should be ruled in black ink. Paper ruled in **green, yellow, or red should not be used** unless it is desired to have all the co-ordinate lines show. Lettering and numerals should be neatly done in India ink preferably with a stencil (**do not use typewriting**) and be of such size that they will be legible and not less than one millimeter in height when reproduced in a cut three inches wide. All experimental points should be carefully drawn with instruments. Illustrations need not be more than two or three times the size of the desired reproduction, but the ratio of height to width should conform with that of the type page. **The original drawings and one set of small but clear photographic copies are to be submitted.**

(ii) *Photographs:*—Prints should be made on glossy paper, with strong contrasts; they should be trimmed to remove all extraneous material so that essential features only are shown. Photographs should be submitted **in duplicate;** if they are to be reproduced in groups, one set should be so arranged and mounted on cardboard with rubber cement; the duplicate set should be unmounted.

(iii) *General:*—**The author's name, title of paper, and figure number should be written in the lower left-hand corner (outside the illustration proper) of the sheets on which the illustrations appear.** Captions should not be written on the illustrations, but typed on a separate page of the manuscript. All figures (including each figure of the plates) should be numbered consecutively from 1 up (arabic numerals). **Each figure should be referred to in the text.** If authors desire to alter a cut, they will be charged for the new cut.

TABLES:—Titles should be given for all tables, which should be numbered in Roman numerals. Column heads should be brief and textual matter in tables confined to a minimum. **Each table should be referred to in the text.**

REFERENCES:—**These should be listed alphabetically by authors' names, numbered in that order, and placed at the end of the paper.** The form of literature citation should be that used in the respective sections of this Journal. **Titles of papers should not be given in references listed in Sections A, B, E, and F, but must be given in references listed in Sections C and D.** The first page only of the references cited in papers appearing in Sections A, B, and E should be given. **All citations should be checked with the original articles.** Each citation should be referred to in the text by means of the key number; in Sections C and D the author's name and the date of publication may be included with the key number if desired.

The *Canadian Journal of Research* conforms in general with the practice outlined in the *Canadian Government Editorial Style Manual*, published by the Department of Public Printing and Stationery, Ottawa.

Reprints

Fifty reprints of each paper without covers are supplied free. Additional reprints, if required, will be supplied according to a prescribed schedule of charges. On request, covers can be furnished at cost.